Ref. Ares(2022)5227646 - 19/07/2022

water mining

water mining
value for society

Deliverable 6.1

Report on the results of the bench-scale tests

Submission Date: 31 December 2021

Revised version: 18 May 2022

This project has received funding from the European Union's Horizon 2020 research and innovation programme under grant agreement 869474.

Deliverable information

Deliverable 6.1	Project management guidelines
Related Work Package	WP6
Deliverable lead	TU Delft
Author(s)	Ali Elahinik, Sarah Koller, Gertraud Kanzler, Maria Kyriazi, Maria Avramidi, Jelica Novakovic, Luca Sbardella, Ieva Sapkaite
Contact	Ali Elahinik
Reviewer	Ellen Tuinman
Grant Agreement Number	869474
Instrument	H2020 – Innovation Action
Start date	1st September 2020
Duration	16 months
Type of Delivery (R, DEM, DEC, Other)[1]	R
Dissemination Level (PU, CO, CI)[2]	PU
Date last update	18 May 2022
Website	www.watermining.eu

History of Changes

Revision no.	Date	Description	Author(s)
0	17-12-2021	Compiled reports	Ali Elahinik
1	22-12-2021	TU Delft revisions	Ali Elahinik
2	23-12-2021	WP Leader review	Ellen Tuinman
3	29-12-2021	Final version	Ellen Tuinman
4	18-05-2022	Revision after reviewing	Ali Elahinik

[1] **R**=Document, report; **DEM**=Demonstrator, pilot, prototype; **DEC**=website, patent fillings, videos, etc.; **OTHER**=other

[2] **PU**=Public, **CO**=Confidential, only for members of the consortium (including the Commission Services), **CI**=Classified

Executive Summary

This deliverable is associated with the implementation of Task 6.1 of Work Package 6. TUDELFT compiled a report (Deliverable 6.1) to summarize the results and conclusions from the various bench-scale tests described under subtasks 6.1.1 and 6.1.2 which provides input for the design of the Industrial mining demo unit to be tested at HEXION and a second demonstration location which is still to be determined. The scope of the deliverables are highlighted in section 2.

In Subtask – 6.1.1, the effect of brine concentration and organic content on the oxidization rate (thus the unit size) as well as raw material consumption, energy use, and heat generation are explored by means of lab- and pilot-scale testing to determine the optimum design for a broader range of industrial cases. The high pressure oxidation experiments (section 3.1) are performed by HEXION and KVT. The evaporation/crystallization experiments (section 3.2) are performed by NTUA and TITANSALT.

In Subtask – 6.1.2, TUDELFT conducts bench-scale experiments using the existing aerobic granular sludge technology (section 4.1) to test its suitability for the treatment organic containing brine originating from HEXION and evaluate the recovery of biopolymer (Kaumera) from the sludge. The results of these studies provide significant inputs for the full-scale study of HEXION as well as for the replication case study for the sugar industry in India. Furthermore, feasibility tests to evaluate the suitability of various commercial membranes for organic solvent recovery from HEXION brine streams are carried out by Eurecat (section 4.2). Techniques explored include pervaporation and vacuum membrane distillation which could be alternatives to thermal separation.

After the completion and submission of the 1st deliverable (D6.1) for the period M1 – M18 on 31st of December 2021, comments were received on the 5th of May 2022 from the project officer and the reviewers. Changes were implemented according to the comments including the addition of the Executive Summary and the tasks and deliverables associated with Work Package 6 and adjustment of some elements in the overall report structure.

List of Figures

Figure 1. Schematic overview of the HPO 4
Figure 2. 3D model of the demo unit, view 1 5
Figure 3. 3D model of the demo unit, view 2 5
Figure 4. Process Flow Diagram of the evaporator 13
Figure 5. 3D Scheme of the MED evaporator 13
Figure 6. Photos of the MED evaporator 14
Figure 7. Photos of the crystallizer 16
Figure 8. Schematic overview of the AGS-SBR operational cycle. 20
Figure 9. Photographic overview of the Aerobic Granular Sludge reactor during aeration (left) and settling phase (right). 22
Figure 10. Graphical representation of floccular sludge (left) in comparison to granular sludge (right). Due to oxygen gradient across the granules (aerobic on the outside and anaerobic on the inside), different microbial communities coexist in different layers (Winkler et al. 2012). 23
Figure 11. Stereoscopic overview of the Aerobic Granular Sludge grown on glycerol. Picture (A) was taken during the initial days of reactor operation, (B) day 37, (C) end of the experimental period day 226, (D & E) shows biomass settling and the settled bed, respectively. The pictures show the washout of the floccular biomass and the formation of dense smooth granules over time. Scale bar equals 1000 µM. ... 25
Figure 12. Concentrations of glycerol (circles) and phosphate (diamonds) throughout a cycle after 85 days of reactor operation. The red-dashed vertical line indicates the switch from the anaerobic to aerobic phase. 25
Figure 13. Concentrations of biodegradable COD (triangle) and glycerol in COD equivalent (circle). The dashed vertical line indicates the switch between anaerobic and aerobic conditions. 26
Figure 14. Fundamental principles of MD process (Shengying et al., 2021). 28
Figure 15. Schematic representation of the four major MD configurations (Pei et al., 2021) 30
Figure 16. Membrane distillation lab equipment and schematic air gap configuration. 32
Figure 17. Thermomixer and vials with different solutions and membrane samples at the beginning of the test. After one week the membranes were withdrawn, dried and prepared for scanning electron microscope (SEM) analysis. This technique, allowing to produce high-resolution images of the membrane's surface morphology, was used to assess the effect of the wastewater and/or MIBK on the morphological properties of the membranes. Before placing membranes inside the microscope, the membrane surfaces were covered with a thin layer of gold to make membrane samples conductive. By fixing the electron beam at a single point in the membrane sample, qualitative and quantitative elemental microanalysis of the constituent elements of the specimen can be performed at that particular volume of interaction, following the method of Energy Dispersive X-Ray (EDX) spectroscopy. This SEM property allows to examine what is present on the membrane surface. 33
Figure 18. ePTFE membrane´s surface after the MD test. 34
Figure 19. SEM images of PTFE membrane. (a) MQ water, (b) wastewater, (c) MQ+MIBK solution 0.4% and (d) wastewater+MIBK solution 0.4% 35
Figure 20. PTFE elemental composition analysis was carried out with EDX method. 36
Figure 21. SEM images of PVDF membrane. (a) MQ water, (b) wastewater, (c) MQ+MIBK solution 0.4% and (d) wastewater+MIBK solution 0.4% 37
Figure 22. Thermomixer and vials with different solutions and membrane samples at the end of the test (one week later). 38
Figure 23. SEM images of UHMwPE membrane. (a) MQ water, (b) wastewater, (c) MQ+MIBK solution 0.4% and (d) wastewater+MIBK solution 0.4% 39
Figure 24. UHMwPE elemental composition analysis carried out with EDX method. 39

List of Tables

Table 1. Description of Hexion brine 6
Table 2. Analysis of Hexion brine 7
Table 3. List of catalysts, temperature, oxygen and brine feed. 8
Table 4. Preparation of synthetic brine 8
Table 5. List of analytical methods 8
Table 6. Lab experiment result 9
Table 7. Pilot-plant experiment 9
Table 8. GC-MS analysis. Polluted brine EEP-106. 9
Table 9. Treated brine 11
Table 10. Wastewater analysis 14
Table 11. Results from the MED experiments 15
Table 12. Results from the crystallizer's operation 17
Table 13. Weight measurement of samples 18
Table 14. Wastewater composition. 31

Table of Contents

Deliverable information i

Executive Summary ii

List of Figures iii

List of Tables iv

1 Overview of the Project 1

2 Scope of the Deliverables 2

3 Subtask – 6.1.1 3

3.1 HEXION & KVT: High-Pressure Oxidation 3

3.1.1 Technology Description 3
3.1.2 Pictures & Schematics 4
3.1.3 Description of the Experiments 6
3.1.4 Results & Discussion 9
3.1.5 Conclusion 11

3.2 NTUA & TITANSALT: Evaporation/Crystallization 12

3.2.1 Technology Description: Evaporator 12
3.2.2 Pictures & Schematics 13
3.2.3 Description of the Experiments 14
3.2.4 Results & Discussion: Evaporator 15
3.2.5 Technology Description: Crystallizer 15
3.2.6 Pictures & Schematics 16
3.2.7 Description of the Experiments 16
3.2.8 Results & Discussion: Crystallizer 17
3.2.9 Comparison of the technologies 17
3.2.10 Possible scaling to the system. 18
3.2.11 Conclusion 18

4 Subtask – 6.1.2 19

4.1 TU Delft: Aerobic Granular Sludge 19

4.1.1 Technology Description 19
4.1.2 Pictures & Schematics 22
4.1.3 Description of the Experiments 23
4.1.4 Results & Discussion 24
4.1.5 Conclusion 26

4.2 Eurecat: Membrane Distillation 28

4.2.1 Technology Description 28
4.2.2 Pictures & Schematics 28

4.2.3 Description of the Experiments 31
4.2.4 Results & Discussion 33
4.2.5 Conclusion 40

4.3 References 41

4.3.1 TU Delft: Aerobic Granular Sludge 41
4.3.2 Eurecat: Membrane Distillation 43

1 Overview of the Project

The WATER-MINING project aims to provide for real-world implementations of the Water Framework Directive (and other water-related legislation), as well as the Circular Economy and EU Green Deal packages by showcasing and validating innovative next-generation water resource solutions at a pre-commercial demonstration scale. These solutions combine WATER management services with the recovery of value-added renewable resources extracted/ MINED from alternative water resources ("WATER-MINING").

The project will integrate selected innovative technologies that have reached proof of concept levels under previous EU projects. The value-added end-products (water, platform chemicals, energy, nutrients, minerals) are expected to provide regional resource supplies to fuel economic developments within a growing demand for resource security. Different layouts for urban wastewater treatment and seawater desalination are proposed, to demonstrate the wider practical potential to replicate the philosophy of approach in widening circles of water and resource management schemes. Innovative service-based business models (such as chemical leasing) will be introduced to stimulate progressive forms of collaboration between public and private actors and access to private investments, as well as policy measures to make the proposed water solutions relevant and accessible for rolling out commercial projects in the future. The goal is to enable costs for the recovery of the resources to become distributed across the whole value chain fairly, promoting business incentives for investments from both suppliers and end-users along the value chain. The demonstration case studies are to be first implemented in five EU countries (NL, ES, CY, PT, IT) where prior successful technical and social steps have already been accomplished. The broader project consortium representation will be an enabler to transferring trans-disciplinary project know-how to the partner countries while motivating and inspiring relevant innovations throughout Europe.

2 Scope of the Deliverables

Within the WATER-MINING project, Work Package 6 (WP6) is about the demonstration of closed-loop water recovery in the industrial sector. WP6 is structured as follows:

- Task 6.1 : Engineering design of the water treatment system for the purification of industrial brine.
- Task 6.2 : Manufacturing and installation of the demo plant.
- Task 6.3 : Operation and optimization of the demo plant/ testing of brine recylcing back to the supplier/ replication to sugar industry in India
- Task 6.4 : Internal WP6 coordination and inter-linkages with other WPs.

The results from the implementation of this WP are presented through 7 deliverables:

- Deliverable 6.1: Report on bench-scale tests (connected to Task 6.1)
- Deliverable 6.2: Engineering drawings (connected to Task 6.1)
- Deliverable 6.3: Operating and maintenance manual (connected to Task 6.2 & 6.3)
- Deliverable 6.4: Report on INDUSTRIAL-MINING demo (connected to Task 6.3)
- Deliverable 6.5: Report on the technical results from the implementation of WP6 - input for interrelated WPs (connected to Task 6.4)
- Deliverable 6.6: Report on the technical results from the implementation of WP6 - input for interrelated WPs (1st update) (connected to Task 6.4)
- Deliverable 6.7: Report on the technical results from the implementation of WP6 - input for interrelated WPs (2nd update) (connected to Task 6.4)

The current report is the first deliverable (D6.1) of WP6 which comprises Subtask – 6.1.1 Detailed engineering for demonstration scale for combined high pressure oxidation and evaporation/crystallization and Subtask – 6.1.2 Wastewater treatment with membranes for solvent recovery and with aerobic granular sludge for the recovery of Kaumera. This deliverable was lead by HEXION and involved KVT, TUDELFT, EURECAT and TITANSALT as partners.

This deliverable is a “public” deliverable, thus not containing any confidential information.

3 Subtask – 6.1.1

3.1 HEXION & KVT: High-Pressure Oxidation

3.1.1 Technology Description

KVT process technology has developed the SEABRINE™ technology for the treatment of contaminated industrial water. It is already successfully implemented in Epichlorohydrin and epoxy resin production plants up to a treatment capacity of 70 m^3/h.
The SEABRINE™ technology aims for maximum energy recovery and low to zero waste. The process is divided into Pre-treatment; High-Pressure Oxidation and catalyst recycling units.

The SEABRINE™ technology is primarily advantageous when very low TOC values as low as 7 ppm are required in the purified brines. Purified sodium chloride brines are recycled in Chlor-Alkali electrolysis plants as raw material.

Within the EU-funded WATER-MINING project, a High-Pressure Oxidation (HPO) Demo Plant was developed. It can handle a mass flow of up to 0.1 m^3/h of raw brine with different degrees of TOC and Salt content. Another aim of the HPO demo plant is to test other materials for the HP equipment and a new concept of catalyst recovery to optimize operational and investment costs for industrial-scale plants.

3.1.1.1 Brine Pre-treatment

In the HPO demo plant, the pH-Value of the Brine is adjusted with hydrochloric acid. Typical pre-treatment steps are filtration and AOX reduction to prevent plugging and corrosion.

3.1.1.2 HPO

The oxidation reaction is a homogenous catalytical reaction. The catalyst is mixed with the brine and the oxidation agent. The brine is pressurized to above 50 bar and preheated in a recuperator up to above 220°C by recovering the heat of the purified brine downstream of the reactor. The final operating temperature is realized by the exothermic oxidation reaction.

The purified brine is depressurized, and the heat is recovered for preheating the raw brine. Depending on the site conditions, further treatment of the gas phase or the brine is implemented. In the HPO Demo Plant, a NaOH Scrubber is installed to remove the HCl from the waste gas.

The oxidation rate is >99%. The brine after the oxidation unit has a TOC value of <7 mg/l, which is within the specification for Chlor-Alkali electrolysis.

3.1.1.3 Catalyst Recycling Unit

The homogenous catalyst is separated from the brine to close the catalyst cycle. The pH value is adjusted, and the brine is treated via sedimentation or filtration and ion exchange up to a limit of <0,1 mg/l. The catalyst from both steps is recycled into the raw brine for oxidation. In the HPO Demo Plant, a new method of catalyst recycling will be tested.

3.1.1.4 Pictures & Schematics

In the first step, the conditioning step, the pH value of the brine is adjusted and the catalyst is added from the catalyst recycling unit. The pressure is increased by a high-pressure pump. The brine is heated next by passing through the recuperator in countercurrent with the treated brine from the oxidation reactor. The inlet temperature of the high-pressure oxidation reactor is controlled with an electrical heater. In the reactor, the TOC is reduced. The treated brine is cooled in the recuperator and depressurized afterward. The catalyst is recycled in two steps in the catalyst recycling unit. In Figure 1 the schematic overview is given.

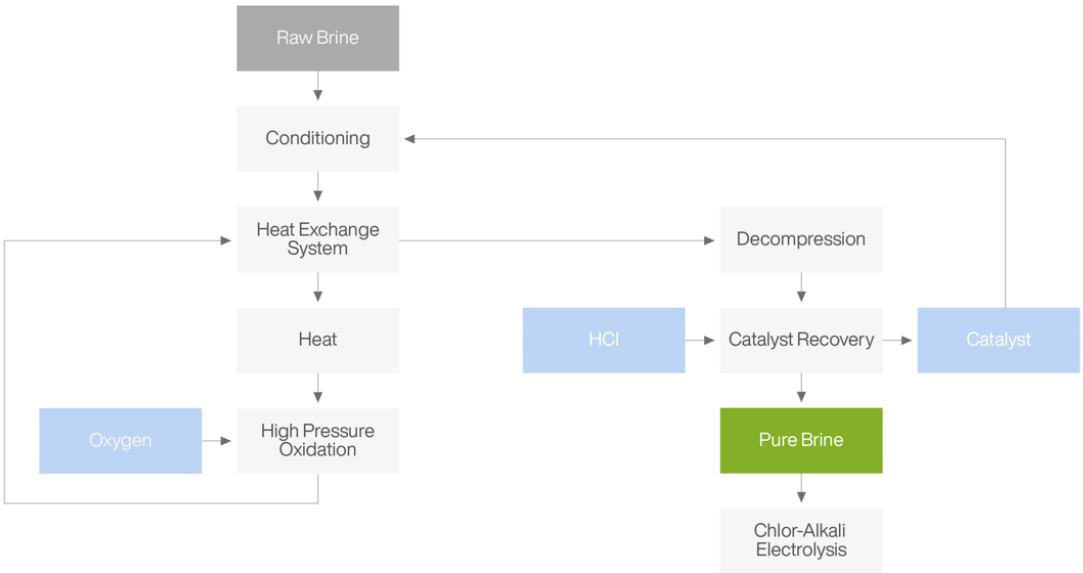

Figure 1. Schematic overview of the HPO

3.1.2 Pictures & Schematics

The illustrations Figure 2 and Figure 3 show the 3D model of the demo unit (status Oct., 19th, 2021). The model was created in NavisWorks.

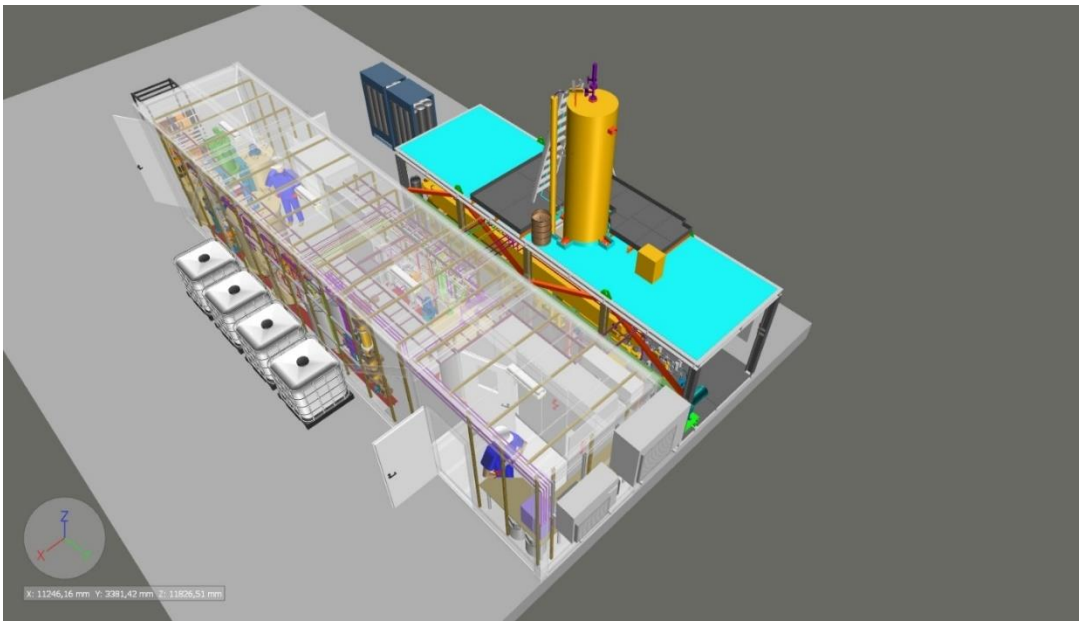

Figure 2. 3D model of the demo unit, view 1

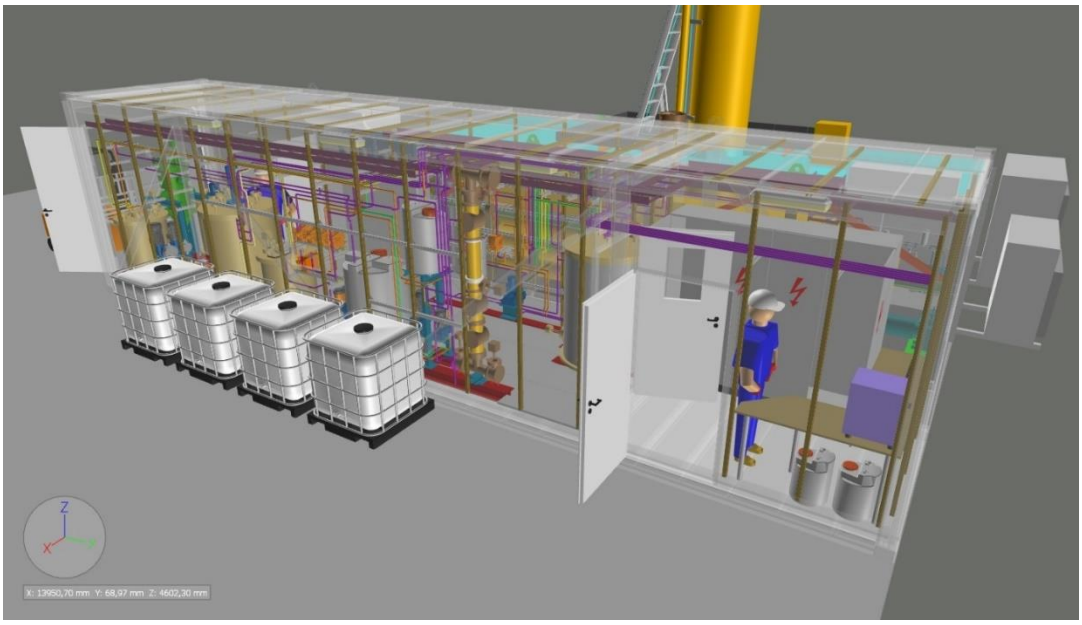

Figure 3. 3D model of the demo unit, view 2

3.1.3 Description of the Experiments

3.1.3.1 Sample Description:

HEXION provided 50 L brine from their liquid resin production. This wastewater had a relatively low salt concentration (approximately 12 wt%). For electrolysis, the salt concentration should be above 20 wt%. Therefore, the brine needs to be concentrated.
The following two options were discussed:

- Wastewater is concentrated before High-Pressure Oxidation. TOC is also concentrated in the brine and TOC is found in the condensate as well.
- Wastewater is concentrated after the High-Pressure Oxidation. TOC of the treated brine is concentrated. To comply with the limit value of below 7 ppm of the electrolysis, the TOC must be degraded nearly completely to about 2 ppm before concentration.

Synthetic brine and original brine were used for the feasibility study. The reaction conditions were first optimized with the synthetic brine and then compared with the original brine. The TOC of the synthetic brine was composed of only Glycerol.

Table 1. Description of Hexion brine

Sample ID (KVT)	EEP-106	
Sample ID (HEXION)	Wastewater LER plant	
Sample received on	15.10.2020	
Sample Appearance		
pH of received sample	12,6	12,6
Sample Description	Turbid white	Turbid white, brownish, some precipitate, when acidified precipitation occurs and clear liquid is formed
Amount of sample	3 x 10 L	2 x 10 L

Table 2. Analysis of Hexion brine

Compound	Unit	EEP-106
NPOC (=TOC)	mg/l	2062 ± 28
NaCl	wt%	11.8
Chloride	mg/l	79.4
pH-value	-	12.56
Organic components	% peak area	See Error! Reference source not found.

3.1.3.2 Lab Experiment

The pH value of brine EEP-106 (250 mL) was adjusted to below 5, and the catalyst (5000 mg/l) was added. 200 ml were discontinuously treated in the lab autoclave with high pressure above 50 bar and high temperature above 200°C. The TOC value of the polluted and the treated sample were measured.

Brine No.		EEP-106
Volume of brine	ml	250
NaCl	%	11.8
NPOC before oxidation	mg/l	2062 ± 28
NPOC after oxidation	mg/l	< 1 mg/L
pH before oxidation	-	< 5

3.1.3.3 Brine Pre-treatment

When the pH value of the original brine EEP-106 was adjusted, a precipitate was formed. The precipitate was removed by filtration.

3.1.3.4 Pilot plant experiment

Synthetic brines with 2000 mg/l and 8000 mg/L TOC were prepared. The pH value was adjusted, and the brine was mixed with the catalyst in the crude brine tank. The brine was continuously pumped into the oxidation reactor with a high-pressure pump. It was mixed with oxygen and heated in the pipe between the pump and reactor. The reactor was electrically heated to the reaction temperature.

Experiments N1101/1 were done with synthetic brine, and N1102 with brine from HEXION (EEP-106).

Table 3. List of catalysts, temperature, oxygen and brine feed.

No.	Duration	Catalyst	Temperatur	Oxygen feed	Brine feed
-	h	mg/l	°C	Nl/h	l/h
N1101/1	10	2000	< 270	35	2.41
N1101/3	5	2000	< 270	35	1.54
N1102/1	14	2062	> 270	35	2.21
N1102/2	5	2062	< 270	35	1.31
N1103/1	8	8000	> 270	50	0.85

Table 4. Preparation of synthetic brine

Parameter		Brine 1	Brine 2
Volume		5 x 20 L	22 L
NaCl	wt%	11.8	21
NPOC before oxidation	mg/L	2000	8000
Glycerol	g/L	5.12	20.5
catalyst	g/L	2000	4000
pH before oxidation	-	< 5	< 5

Table 5. List of analytical methods

Parameter	**Method**
Qualitative Analysis of TOC	Shimadzu GCMS-QP2010 Ultra EI / Zebron ZB-1 (Sample is acidified to pH=1 for measurement) (C1.1rev1)
TOC/IC	InnovOx Analyser (Supercritical water oxidation technique) (C10)
Chloride	Titration according to Mohr (C13)

3.1.4 Results & Discussion

Table 6. Lab experiment result

Experiment	Catalyst	T	TOC polluted brine	TOC product
	mg/l	°C	mg/l	mg/l
1	5000	< 270	2062	< 1

Table 7. Pilot-plant experiment

Experiment	Brine	TOC inlet	T	Brine Flow	TOC outlet
No.	-	mg/l	°C	l/h	mg/l
N1101/1	Synthetic	2000	< 270	2.41	15.1
N1101/3	Synthetic	2000	< 270	1.54	5.58
N1102/1	Wastewater LER plant	2062	> 270	2.21	4.8
N1102/2	Wastewater LER plant	2062	< 270	1.31	5.08
N1103/1	Synthetic brine	8000	> 270	4.2	5.25

Table 8. GC-MS analysis. Polluted brine EEP-106.

Compound	Retention time	Area
	min	%
Methyl Isobutyl Ketone	5.596	5.24
2-Chloro-2-propen-1-ol	6.286	0.19
1,3-Dioxan-5-ol	8.243	0.20
Allyl acetate	8.839	0.18
2,5-Furandione, 3-methyl-	9.618	0.43
Glycerin	10.447	78.75
Succinic anhydride	11.586	0.75
1,4:3,6-Dianhydro-.alpha.-d-glucopyranose	14.015	1.58
p-Dioxane-2,5-dimethanol	14.708	0.47
1,4-Dioxane-2,6-dimethanol	15.079	2.49
1,4-Dioxane-2,6-dimethanol	15.304	9.49

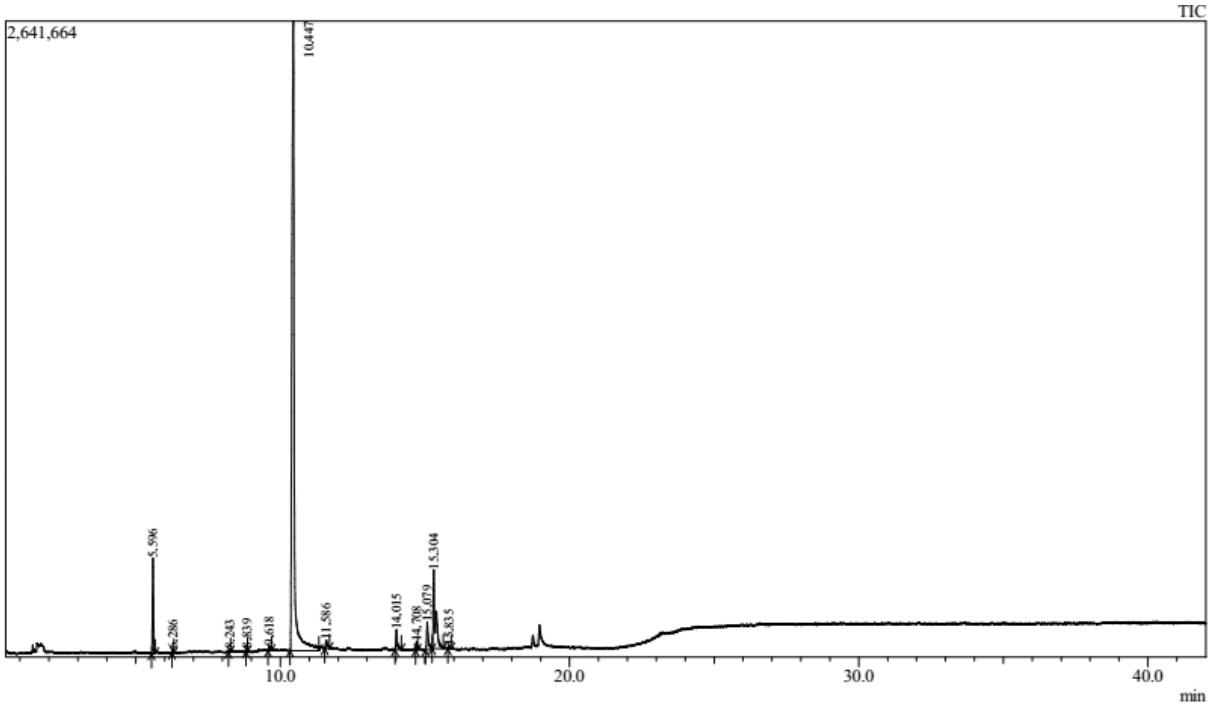

Treated brine (N1102/2):

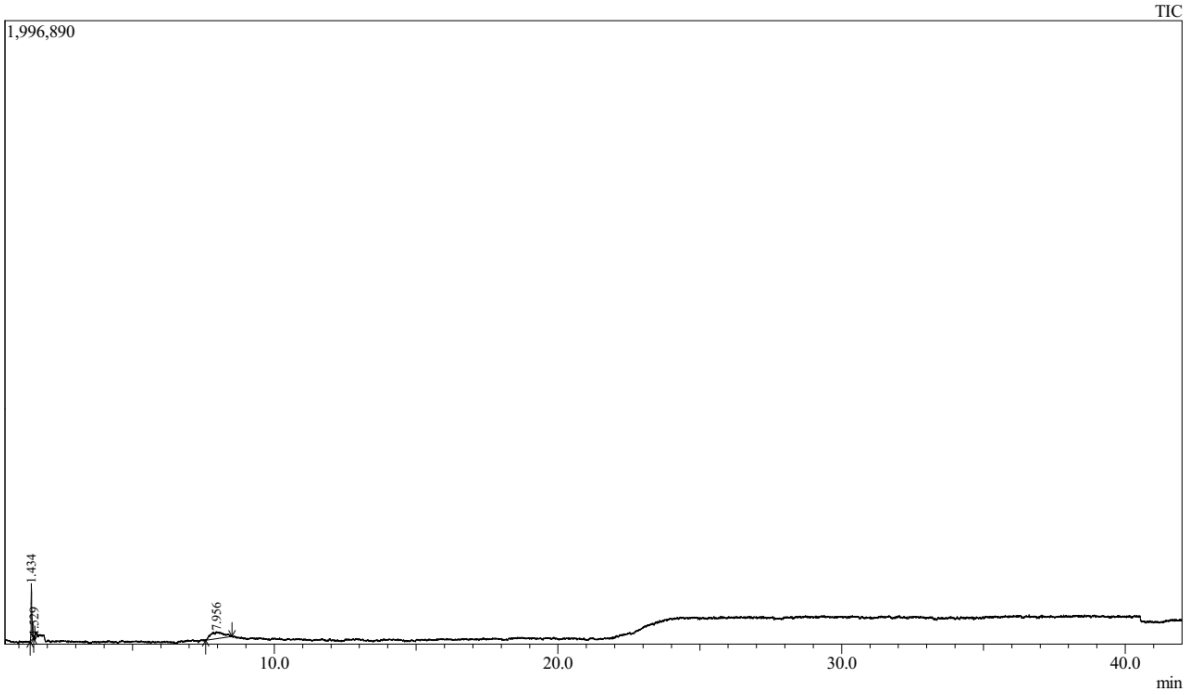

Table 9. Treated brine

Compound	Retention time	Area	Hit
	min	%	%
Carbon dioxide	1.434	34.41	96
Formaldehyde	1.529	64.51	92
Hydrogen chloride	7.956	10.31	90

3.1.5 Conclusion

Synthetic brine and brine from the HEXION plant were treated in a 300 ml Lab Autoclave and a pilot plant with a feed flow rate of 1-2 l/h. The feasibility was tested and parameters were determined for the scale-up of the pilot plant for the WATER-MINING Project. The brine sample from HEXION contained 11.8 wt% NaCl and 2000 mg/l TOC. The parameters in the pilot plant were optimized for this low salt and low TOC brine. Afterward also a sample with 21 wt% NaCl and 8000 mg/l TOC was tested to guarantee that also the TOC in high salt brines can be treated below 7 ppm within the operating parameters of the pilot plant.

The TOC of the synthetic brine was composed only of glycerine and NaCl. The comparison of experiments N1101/3 and N1102/2 showed that the original brine from HEXION needed a reduced brine flow and longer residence times respectively to destruct the TOC below 7 mg/l. The brine with 8000 mg/l was successfully treated as well.

3.2 NTUA & TITANSALT: Evaporation/Crystallization

3.2.1 Technology Description: Evaporator

Multi-Effect Distillation (MED) is a thermal-based technology, widely used in the desalination industry, capable of treating high salinity feeds with high volumes of brine resulting in high water quality.

The MED evaporator used in WP6 for bench-scale experiments has a $2m^3$/day capacity. More specifically, it consists of 2 effects with heat exchangers. Plate heat exchangers are installed in the system, for pre-heating the feed brine and for condensing the produced vapor. An electrical boiler supplies steam to the first effect. The system operates below atmospheric pressure and the brine is sprayed to the first effect on top of the bundle. Hot water from the boiler is running through the heat exchangers of the first effect transferring heat to the feed brine, resulting in water evaporation and brine concentration. Vapor generated by the first effect is transferred to the heat exchangers of the second effect. Thus, the necessary heat for brine vaporization in the second effect is provided by internal heat gain, resulting in energy recovery. The concentrated brine from the first effect is directed towards the second effect for further concentration. In addition, the concentrated brine stream from the second effect is recirculated back to the first effect until the target concentration is achieved, creating this way a close loop. The vapor stream produced by the second effect is used for preheating the inlet brine passing through a heat exchanger and then it is condensed in a plate heat exchanger.

The control of the system is accomplished via a PC-based supervisory control and data acquisition (SCADA) interface. Multiple temperatures, pressure, and flow transmitters are connected in many positions within the system, receiving all the important data for process control. The overall control and monitoring can be achieved using SCADA. All data is collected and controlled using a programmable logic controller (PLC). The aim of the automation system is to display and record information related to the processes, the operation of the equipment, etc. The Process Flow Diagram (PFD) of the MED evaporator unit is shown in Figure 4.

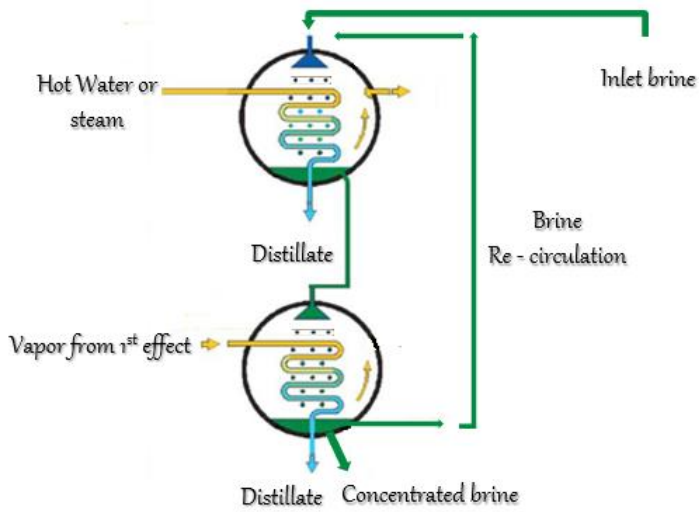

Figure 4. Process Flow Diagram of the evaporator

3.2.2 Pictures & Schematics

In Figure 5, a 3D scheme of the equipment is presented while in Figure 4 the interior of the system container is shown.

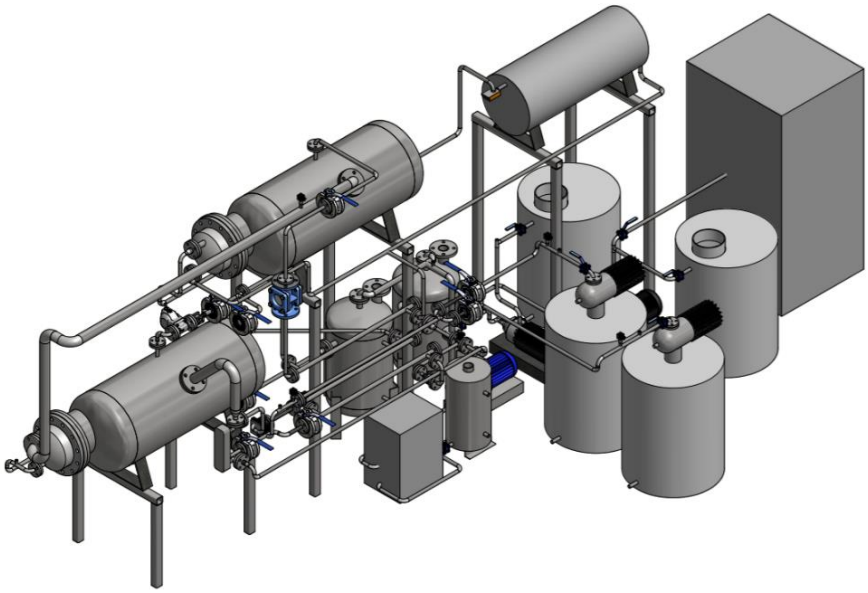

Figure 5. 3D Scheme of the MED evaporator

Figure 6. Photos of the MED evaporator

3.2.3 Description of the Experiments

NTUA prepared synthetic brine solutions for the experiments according to the presented concentrations in Table 10, by dissolving Sodium Chloride in tap water. NTUA performed three experiments for each scenario. In the first scenario the inlet brine salinity was 7%, in the second scenario 12% and in the final scenario 15% targeting the 20% w/w NaCl concentration at the end of the process.

Table 10. Wastewater analysis

	TOC mg/L	COD mg/L	Inorganic Chlorine mg/L	Methyl isobutyl ketone mg/L	TSS (pH8) mg/L	NaCl (calc) wt%
min	590	1550	48000	0	16	7%
mean	1458	4475	79389	71	97	12%
max	3100	8340	99000	260	490	15%

Each experiment lasted 4 hrs, in order to achieve the required concentration and the energy consumption was measured via a PC-based supervisory control and data acquisition (SCADA) interface. The average value of measured parameters for the three scenarios is presented in Table 11.

Table 11. Results from the MED experiments

	7% wt NaCl	12% wt NaCl	15% wt NaCl
Feed Na (g/L)	27,5	47,8	59,1
Feed Cl (g/L)	42,3	73,8	91,2
Condensate Na (mg/L)	22,2	23,8	21,3
Condensate Cl (mg/L)	34,3	36,7	32,9
Concentrate Na (g/L)	81,1	86,1	82,7
Concentrate Cl (g/L)	124,9	132,9	127,7
TDS inlet (g/L)	69,8	121,7	150,3
TDS concentrate (g/L)	205,9	219,1	210,4
Inlet volume (L)	100	100	100
Condensate volume (L)	70	40	25
Concentrate volume (L)	30	60	75
Concentration factor	3,0	1,8	1,4
Water recovery	70%	40%	25%
Energy consumption (KWh/m^3 cond.)	493	574	589

3.2.4 Results & Discussion: Evaporator

During the evaporator operation, two streams are produced, a condensate vapor (water of high quality) and a concentrated brine stream. The inlet brine has been concentrated 1.5 to almost 3 times and water recovery between 30% to 70% is achieved.

The system is powered by electricity. The energy consumption has been calculated per m^3 of condensate produced. Analysis of energy consumption data after each operation of the unit shows that energy consumption is approximately between $490kWh/m^3$ to $590kWh/m^3$.

3.2.5 Technology Description: Crystallizer

The NTUA BEC crystallizer has also been used for another set of experiments. The crystallizer is a concentrator that distillates liquids at low temperatures through the combined effect of vacuum technology and heat pumping. Through a circuit, the heat pump carries out the expansion and compression of the Freon gas and yields both the necessary calories for the evaporation of the liquid and the necessary frigories for its condensation. A thermal exchange takes place in the lower part of the boiling chamber and vapors are condensed in the condenser. The distillate is drawn from the receiver and pumped through the ejector to create a vacuum. The pressure variation produced is sufficient to extract both the concentrate and

the distillate. The energy consumption has been measured by the electrical panel of the system. The crystallizer can treat 0,2m^3/day.

3.2.6 Pictures & Schematics

In Figure 7 some photos of the equipment are presented.

Figure 7. Photos of the crystallizer

3.2.7 Description of the Experiments

The set of experiments performed with the evaporator was repeated using the crystallizer. The operational hours depended on the inlet brine concentration. The first scenario experiments lasted 14hrs while the duration of the second and third scenario experiments was approximately 7hrs. The average values of the experimental results are shown in the table below.

Table 12. Results from the crystallizer's operation

	7% wt NaCl	12% wt NaCl	15% wt NaCl
Feed Na (g/L)	27,5	47,8	59,1
Feed Cl (g/L)	42,3	73,8	91,2
Condensate Na (mg/L)	23,0	23,8	21,3
Condensate Cl (mg/L)	35,5	36,7	32,9
Concentrate Na (g/L)	80,4	86,8	89,8
Concentrate Cl (g/L)	124,1	134,0	138,7
TDS inlet (g/L)	69,8	121,7	150,3
TDS concentrate (g/L)	204,5	220,8	228,5
Inlet volume (L)	100	100	100
Condensate volume (L)	66	45	34
Concentrate volume (L)	34	55	66
Concentration factor	2,9	1,8	1,5
Water recovery	66%	45%	34%
Energy consumption (KWh/m^3 cond.)	845	908	950

3.2.8 Results & Discussion: Crystallizer

Two streams are produced during the crystallizer operation, a condensate vapor (water of high purity) and a concentrated brine stream. In order to achieve the required concentration (20%), a concentration factor between 1,50 and 2,91 and water recovery between 30% and 70% have been achieved. The energy consumption has been calculated per m^3 of condensate produced. Analysis of energy consumption data after the end of experiments shows that energy consumption was approximately between $850kWh/m^3$ and $950kWh/m^3$.

3.2.9 Comparison of the technologies

The evaporator and the crystallizer use the same operating principles. They both operate under vacuum and recirculation. In general, they can produce the same concentration level. The tested crystallizer has shown higher energy consumption than the evaporator. In addition, the tested crystallizer needs quite more operating hours to achieve the same concentration factor as the evaporator. The MED evaporator with a higher capacity and the possibility to work with renewable energy is considered more suitable for the treatment of higher brine flows. The crystallizer could be a suitable option for the treatment of smaller quantities of high concentrated brine (more than 15% TDS).

3.2.10 Possible scaling to the system.

The MED evaporator used for the bench-scale tests is a batch operating system. The inlet brine is passing through the two effects and recirculates until reaches the required concentration. The system is closed and it is not possible to evaluate the possibility of scaling inside the effects. It is constructed of a super duplex (Stainless Steel, AISI316 (1.4401)) a corrosion-resistant material. The possibility of scaling formation (a frequent operational problem of evaporators) was tested by immersing Super duplex samples 5 x 2 cm (length x width) in 12% wt NaCl solution. The samples were left in this solution at 70°C for 4 months. The synthetic brine solution for two samples was prepared with distillate water and sodium chloride and for the other two samples with tap water and sodium chloride. Also, in two additional samples, glycerin (0.3%) was added, in order to simulate the brine from HEXION's Pernis Plant. Table 13 present the results of the weight measurements of the samples before and after immersion.

Table 13. Weight measurement of samples

	Weight beginning (g)	Weight after the 4 months (g)
Sample with distillate water and NaCl.	17,9769	17,9752
Sample with distillate water and NaCl	16,9456	16,9445
Sample with tap water and NaCl	18,5753	18,5774
Sample with tap water and NaCl	17,4893	17,4897
Sample with distillate water, NaCl, and glycerin	19,1092	19,1075
Sample with tap water, NaCl, and glycerin	17,4480	17,4460

3.2.11Conclusion

In general, no significant weight and surface changes were observed. Some slight weight losses were noticed for the samples immersed in distillate water solution indicating minor corrosion. On the other hand, a slight weight increase occurred in the samples immersed in tap water solution indicating some scaling formation. The addition of glycerin in the solutions seems that it did not affect the corrosion and scaling of samples.

4 Subtask – 6.1.2

4.1 TU Delft: Aerobic Granular Sludge

4.1.1 Technology Description

The Aerobic Granular Sludge (AGS) process is a novel biological wastewater treatment technology applied for the treatment of both domestic and industrial wastewaters (Bengtsson et al., 2018; Corsino et al., 2015). By applying selective environmental pressures and adjusting the operational conditions, the biomass is stimulated to grow in a granular form with excellent settling properties that reduce the solid-liquid separation time significantly. Furthermore, due to the coexistence of different microorganisms, simultaneous conversions take place within the granules themselves, eliminating the need for having multiple tanks. Because of these distinct advantages compared to the Conventional Activated Sludge (CAS) processes, the AGS reactors have a much smaller footprint and the energy costs can be reduced while maintaining a good effluent quality (Haaksman et al., 2020).

Industrial wastewaters often have properties with unknown effects on the biology of wastewater treatment plants. Although AGS and CAS systems share similar fundamental properties in terms of conversions, in CAS systems the external stress generally has a more pronounced effect on the biomass activity. The biofilm structure of the granules provides an advantage compared to flocculent biomass since the reduced activity can be partly compensated by the activity of the biomass in the depth of the biofilm. This was illustrated in the work of de Kreuk et al. (2005) showing that lower activity due to decreased temperature was compensated by larger aerobic volume of the granules resulting from increased oxygen penetration depth. Moreover, the oxygen and substrate gradient across the biofilm provides several niches that promote microbial diversity, which in turn can enhance the functional stability of the treatment process (Winkler et al., 2013).

There are several parameters that are important for obtaining stable and smooth granules. One of which is the selection of slow-growing microorganisms such as Polyphosphate Accumulating Organisms (PAO) and Glycogen Accumulating Organisms (GAO) that form dense smooth granules (de Kreuk & van Loosdrecht, 2004). When biodegradable organic carbon (mainly volatile fatty acids) is supplied to the system under anaerobic conditions, it is converted by certain microorganisms (PAOs for instance) into storage polymers known as Poly-Hydroxy-Alkanoates (PHA) (Oehmen et al., 2005). In the subsequent aerobic phase, the stored organic carbon is then oxidized to provide energy for the formation of biomass and glycogen and phosphorus replenishment (Oehmen et al., 2007; Pronk et al., 2015). Thus, the anaerobic feeding and storage select for slow-growing microorganisms that are essential for AGS system stability and performance.

$$\textbf{Anaerobic phase}: Organic\ carbon \rightarrow Storage\ polymers\ (PHA)$$

$$\textbf{Aerobic phase}: Storage\ polymers \rightarrow Biomass$$

A typical AGS cycle includes anaerobic plug-flow feeding, aerobic mixing, and a short settling time (Figure 8).

- The anaerobic plug-flow feeding from the bottom of the reactor ensures a high substrate concentration throughout the sludge bed. This feeding strategy also promotes the formation of larger granules to settle at the bottom of the reactor and to be the first in contact with the substrate.
- During the aeration phase, oxygen is supplied to the system for oxidation.
- A short settling time is then applied to ensure the retention of granular biomass with fast settling velocities and the discharge of floccular aggregates with poor settling properties.

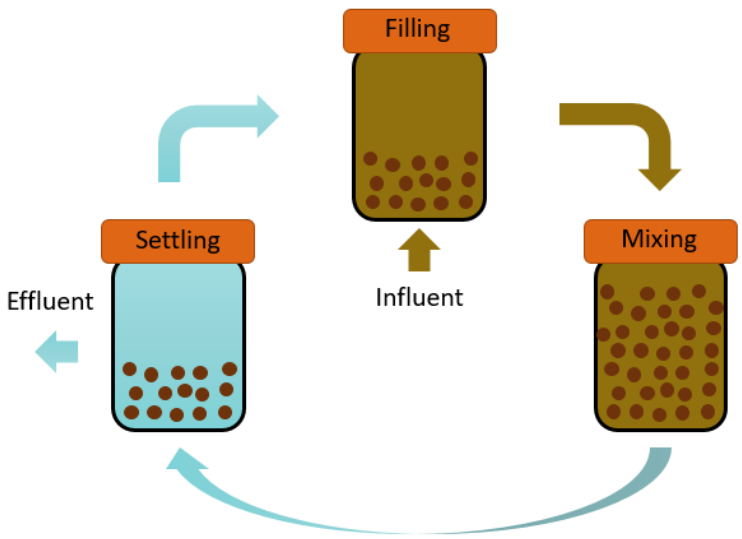

Figure 8. Schematic overview of the AGS-SBR operational cycle.

The AGS technology was developed by the Delft University of Technology in the Netherlands and is commercially known as Nereda® which is the product of Royal HaskoningDHV. Currently, there are over 80 wastewater treatment plants globally that have adopted the Nereda® technology ranging from 5,000 to 2,400,00 P.E.

One of the products that can be recovered from AGS is Extracellular Polymeric Substances (EPS) which is commercially known as Kaumera. In line with the concepts of sustainability and circularity, Kaumera can be regarded as an environmentally friendly biodegradable polymer with vast potential applications. In 2020, two full-scale demonstration sites in the Netherlands (in Epe and Zutphen) have been commissioned for Kaumera recovery from the granular sludge of Nereda® Waste Water Treatment Plants (WWTP). While Kaumera extraction has a positive effect on energy consumption and CO_2 emissions, it also reduces the sludge mass by 20-35%.

EPSs are gel-like microbial secretions that play a crucial role in the formation and structural stability of microbial aggregates. These complex matrices are mainly composed of polysaccharides, proteins, nucleic acids, humic substances, and intercellular polymers (Felz et al., 2016; Zeng et al., 2016). The secretion of these biopolymers evokes cell-to-cell adhesion which is important for the formation of AGS.

Currently, different techniques exist for the extraction of Kaumera and the choice of the extraction method not only influences the quantity but also the properties of the EPS (Felz et al., 2016). Therefore, the extraction method should be selected based on the intended industrial applications. At the moment, Kaumera in the industry is harvested via extraction at high temperatures (≈80 °C) and alkaline conditions (pH 9 – 11). Using centrifugation, the residual sludge is separated from the Kaumera-containing solution. The solubilized Kaumera is then precipitated under acidic conditions (pH 2 – 3) and at the temperature of 25 °C. Lastly, Kaumera is harvested via a final centrifugation step in the form of a stable ionic gel.

4.1.1.1 Scope of the Bench-scale test

HEXION wastewater composition was analyzed by KVT and glycerol was found to be the main contributor to the TOC which was also confirmed by HEXION. Therefore, the experiments were performed with glycerol as the sole carbon source to investigate whether stable granulation could be obtained while evaluating the carbon and nutrient removal capability of the system.

Although a significant body of research exists on the performance of AGS with Volatile Fatty Acids (VFA) as the carbon source (mainly acetate and propionate), very few studies have focused on using rather unconventional sources of carbon such as sugars and alcohols. To the best of the author's knowledge, there has been no research on the effect of glycerol on AGS and the selection of the microbial community. The main question is if the glycerol is directly accumulated by PAO or fermented first. If it is fermented, 1,3-propanediol is a likely fermentation byproduct. There is a large chance that this will not be sequestered anaerobically, resulting in aerobic COD conversion that might negatively influence the granular sludge formation. If other bacteria than PAO are selected a different EPS might be formed with different properties than Kaumera.

To further emphasize the importance of this research, glycerol is also a waste product of many different industrial processes such as biodiesel production (Pinto & De Araujo Mota, 2014). For instance, production of every 10 kilograms of biodiesel generates about 1 kilogram of glycerol (Plácido & Capareda, 2016). Due to its abundance and relatively cheap price, the use of glycerol has attracted the attention of different engineering communities for various applications. Therefore, the outcome of this research provides information that is potentially also relevant for other industries, beyond the scope of this project.

Furthermore, since the wastewater from HEXION also contains a significant amount of NaCl (>10%), separate research will be carried out to distinguish the effect of NaCl on AGS system stability and performance. So far, based on previous research and information available in the

literature, we can confirm that AGS systems can perform stably with a salinity of up to 3% saturation (Bassin et al., 2011; de Graaff et al., 2020). However, these studies have been performed with acetate as the carbon source and whether the same results could be obtained with glycerol as the carbon source requires further research. It is worth noting that successful granulation and stability at salinities of 8% (Ibrahim et al., 2020) and 12% (Sarvajith & Nancharaiah, 2020) have been also reported. The impact of salts, and the maximal tolerable concentration, will be tested in a later stage after we have confirmed that glycerol can result in stable aerobic granular sludge dominated by PAO's that can generate Kaumera type of exopolymers.

4.1.2 Pictures & Schematics

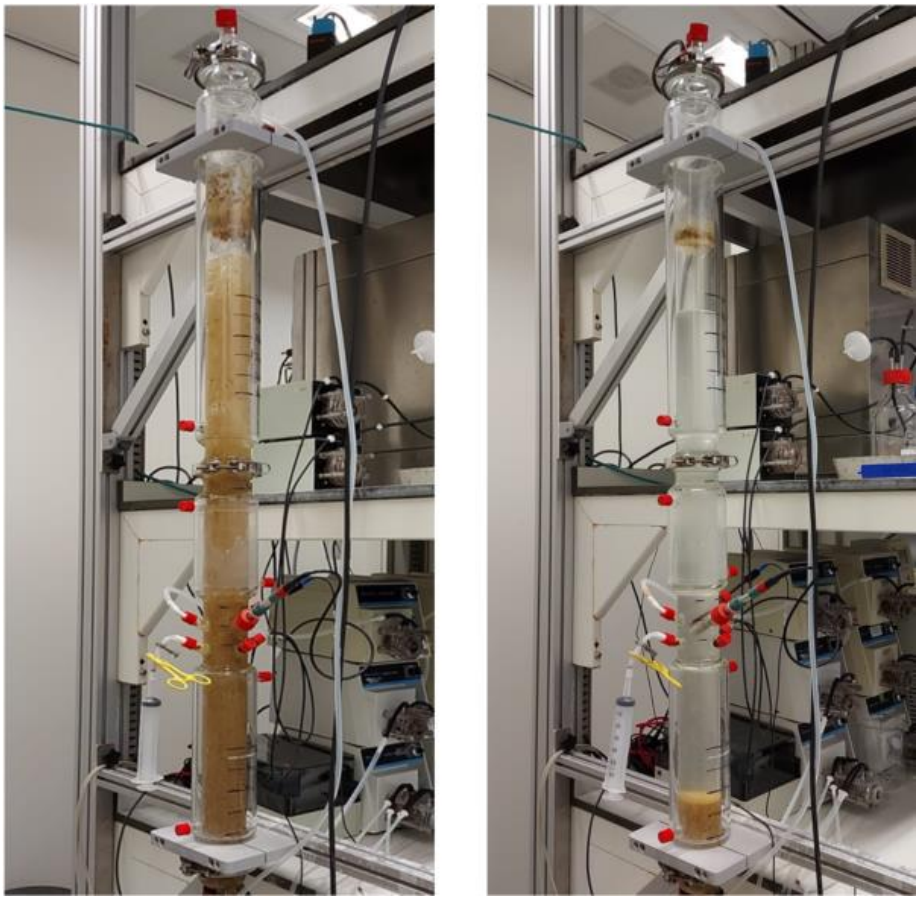

Figure 9. Photographic overview of the Aerobic Granular Sludge reactor during aeration (left) and settling phase (right).

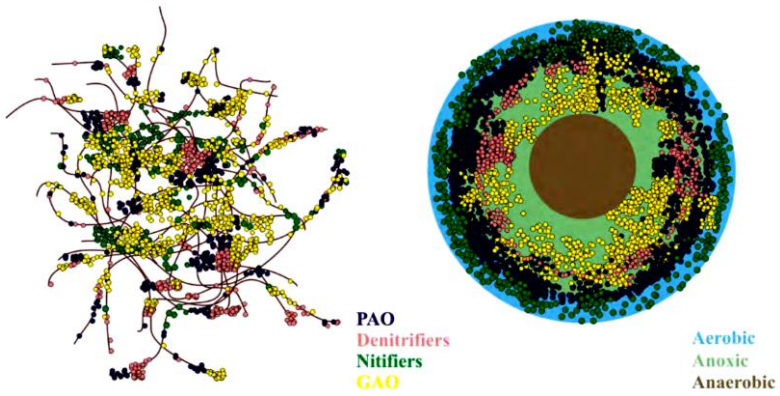

Figure 10. Graphical representation of floccular sludge (left) in comparison to granular sludge (right). Due to oxygen gradient across the granules (aerobic on the outside and anaerobic on the inside), different microbial communities coexist in different layers (Winkler et al. 2012).

4.1.3 Description of the Experiments

The experiments were conducted in a bubble column reactor and operated in an SBR configuration. The working volume of the reactor was 2.8 L with an internal diameter of 5.6 cm and a total height of 90 cm. After effluent withdrawal, 1.3 L remained in the reactor after each cycle representing a volumetric exchange ratio of roughly 54%. The pH was controlled at 7 ± 0.1 by either doing 1M NaOH or 1M HCl. The Dissolved Oxygen (DO) was kept at 50% saturation by a controlled mixture of nitrogen gas and air. The temperature was not controlled. The reactor was seeded with aerobic granular biomass from a pilot-scale wastewater treatment reactor located in Harnaschpolder, the Netherlands.

The influent was 1500 mL consisting of 1200 mL of demineralized water, 150 mL of medium A and 150 mL of medium B. Medium A contained 35.7 mM glycerol, 3.6 mM MgSO4.7H2O, and 4.7 mM KCl. Medium B contained 41.1 mM NH4Cl, 1.95 mM K2HPO4, 1.98 mM KH2PO4, 0.6 mM Allythiourea (ATU) to inhibit nitrification and 10 mL/L of trace element solution. The trace element solution contained 4.99 g/L FeSO4.7H2O, 2.2 g/L Zn.SO4.7H2O, 7.33 g/L CaCl2.2H2O, 4.32 g/L MnSO4.H2O, 2.18 g/L Na2MoO4.2H2O, 1.57 g/L CuSO4.5H2O, 1.61 g/L CoCl2.6H2O and 50 g/L EDTA. The combination of these feed streams resulted in an influent concentration of 400 mg/L Chemical Oxygen Demand (COD), 57.6 mg/L Ammonium (NH4+-N), and 12.2 mg/L of Phosphate (PO4-3-P).

The reactor cycles consisted of 5 min of nitrogen sparging to ensure an anaerobic condition prior to feeding followed by 5 min of feeding, 60 min of nitrogen sparging, 120 min of aeration, 5 min of settling, and 5 min of effluent withdrawal. The off-gas was recirculated with a flow of 5 L/min to keep a steady DO concentration.

All samples were filtered with a 0.45 µm Millipore filter prior to measurement. COD was measured with a spectrophotometer cuvette system (DR 2800, Hach Lange, USA). PO_4^{-3}-P concentration was measured by a Discrete Analyzer (Thermo Fisher Scientific, USA). Glycerol

concentration was measured with an Enzymatic Assay Kit (K-GCROL, Megazyme, Ireland). Pictures of the granules were taken with a stereo zoom microscope (Leica Microsystems Ltd, M205FA, Germany).

4.1.4 Results & Discussion

An AGS-SBR was operated with glycerol as the sole carbon source. The inoculum initially had a dark color since it was obtained from a municipal WWTP. After weeks of reactor operation with glycerol medium and the formation of new biomass, the sludge color changed to light brown. The settling time was then step-wise decreased from 20 to 5 minutes within 4 weeks of operation. Consequently, the effluent became clearer and the floccular biomass was washed out of the system. Once granular biomass formation was visually apparent, the Solids Retention Time (SRT) of 20 days was maintained by manual sludge removal. After the reactor reached a pseudo-steady-state, a low Sludge Volume Index (SVI_5) of 19 mL/g was obtained from the sludge settled bed in the reactor after 5 minutes of settling which indicated an excellent sludge settleability (de Kreuk & van Loosdrecht, 2004).

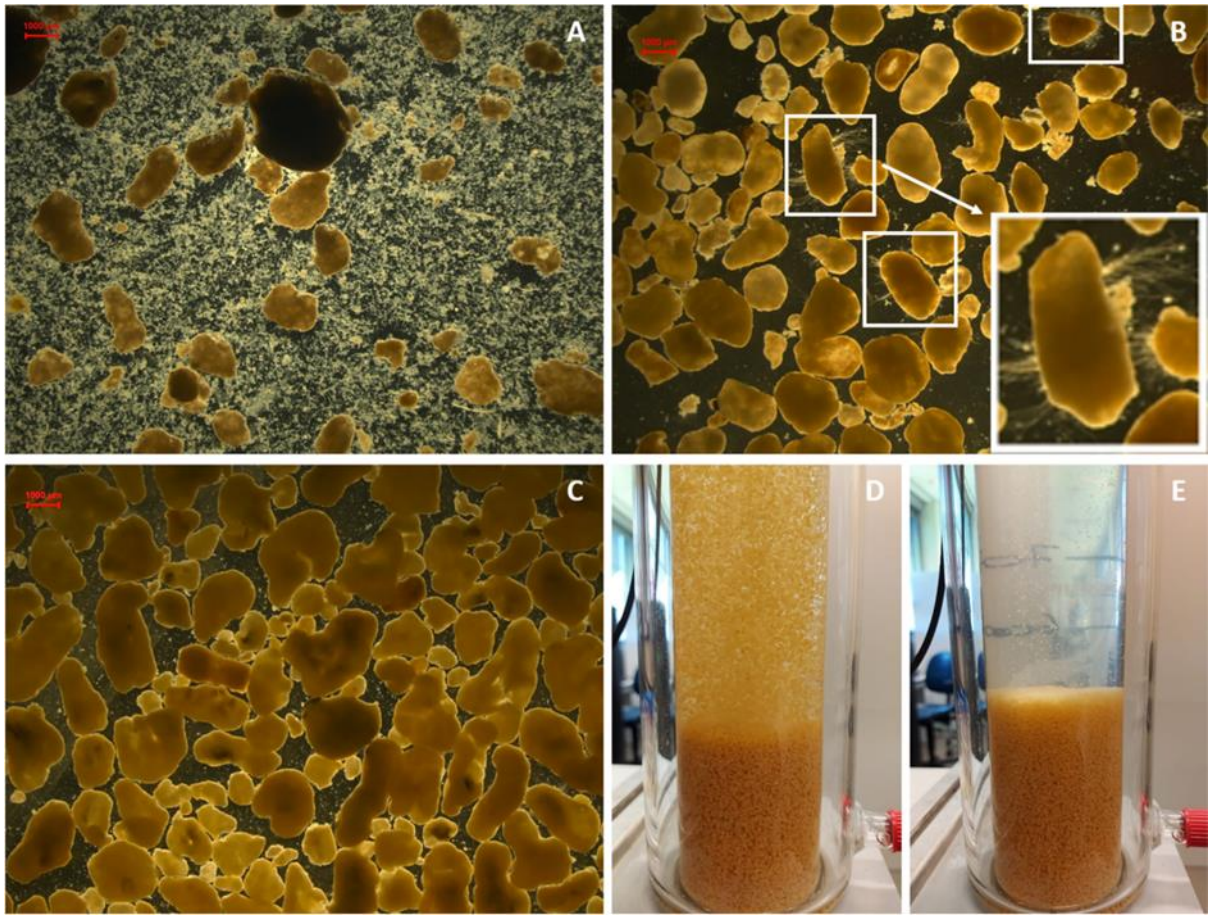

Figure 11. Stereoscopic overview of the Aerobic Granular Sludge grown on glycerol. Picture (A) was taken during the initial days of reactor operation, (B) day 37, (C) end of the experimental period day 226, (D & E) shows biomass settling and the settled bed, respectively. The pictures show the washout of the floccular biomass and the formation of dense smooth granules over time. Scale bar equals 1000 µM.

Figure 12. shows the concentrations of glycerol and phosphate during a typical cycle after 85 days of reactor operation. It can be seen that glycerol is completely removed during the 60 minutes of the anaerobic phase. Coupled with the complete anaerobic glycerol removal, a significant phosphorus release of 65.43 mgP/L was also observed which indicates the suitability of glycerol as a carbon source for Enhanced Biological Phosphorus Removal (EBPR) processes. In EBPR systems, net phosphate removal is achieved by wastage of sludge enriched with poly-phosphate.

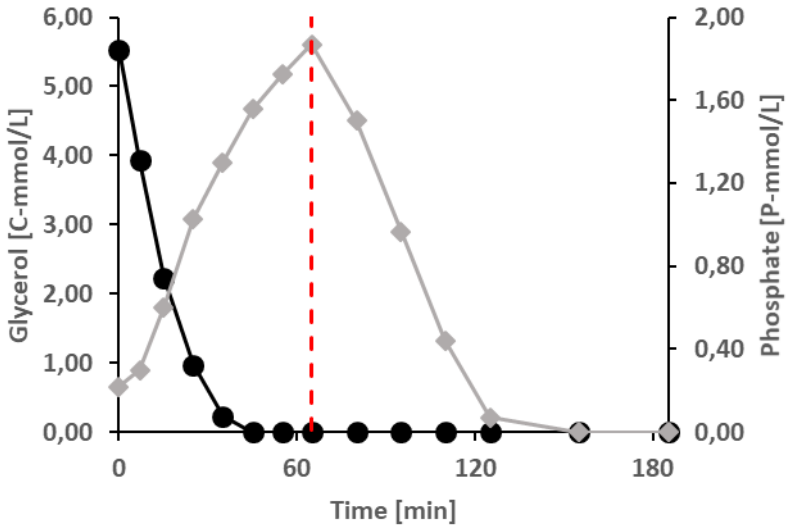

Figure 12. Concentrations of glycerol (circles) and phosphate (diamonds) throughout a cycle after 85 days of reactor operation. The red-dashed vertical line indicates the switch from the anaerobic to aerobic phase.

As shown in Figure 13, although the glycerol was found to be completely removed anaerobically, a fraction of the COD was removed aerobically. This difference points to the anaerobic conversion of glycerol into other compounds that are not taken up anaerobically and are immediately oxidized in the subsequent aerobic phase. These compounds have not yet been identified but are currently under investigation. Based on the information available in the literature, the anaerobic conversion of glycerol using mixed microbial cultures can yield different products such as propionate (Chen et al., 2016; Yuan et al., 2010) or 1,3-propanediol and acetate (Temudo et al., 2008). The formation of VFAs such as acetate or propionate is not problematic for AGS since they can be taken up and converted into storage polymers anaerobically. However, whether the same would hold true with 1,3-propanediol or other potential byproducts as carbon substrate is still not known.

Although about 25% of the COD was converted aerobically, smooth and stable granules were formed (Figure 13). The rapid aerobic uptake of the remaining COD indicates that it is likely primarily converted to storage compounds, which are subsequently used for growth. Pronk et al., (2015) also showed that propanol left over after the anaerobic feeding did not lead to granule instability or irregular outgrowth.

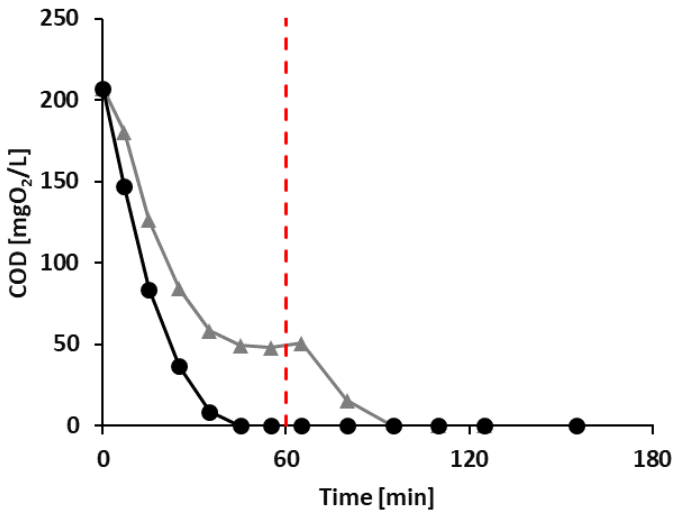

Figure 13. Concentrations of biodegradable COD (triangle) and glycerol in COD equivalent (circle). The dashed vertical line indicates the switch between anaerobic and aerobic conditions.

Now, whether glycerol is directly utilized or first fermented and then utilized in the anaerobic phase is currently being investigated. We hypothesize that glycerol is initially degraded to PAO/GAO-utilizable products and then converted into storage polymers since glycerol is completely removed anaerobically but the biodegradable COD is partly removed aerobically (Figure 13). This hypothesis is also in agreement with the results obtained in a similar study done by Guerrero et al. (2012) where glycerol was used as the sole carbon source in an EBPR system.

4.1.5 Conclusion

Stable granulation with glycerol as the sole carbon source was shown successful. The system has performed stably during the experimental period and complete anaerobic glycerol removal within a cycle was observed. Granulation by PAO has been observed which also indicates that the EPS produced will have the same characteristic as the Kaumera produced in municipal wastewater treatment.

Since it was demonstrated that granulation could be achieved with glycerol, further investigations will be carried out to evaluate the system performance at elevated NaCl concentration dictated by the wastewater composition from HEXION. Some of the challenges associated with conducting experiments at elevated NaCl concentrations are the interference of salt with analytical measurements. Therefore, the experiments should be designed with complications in hindsight. Moreover, elevated NaCl concentrations may inhibit the biological activity of the AGS systems and deteriorate the structure of the granules. One strategy to overcome this challenge is to bio-augment the system with halophilic microorganisms. It is also likely that NaCl alters the EPS properties and thus further investigations are required to characterize the extracted EPS.

4.2 Eurecat: Membrane Distillation

4.2.1 Technology Description

Membrane distillation (MD) is a thermally-driven membrane-based separation technique, which has shown the great potential use for molecular separation in different processes like wastewater treatment and desalination. The prominent mechanism of separation in this technology is only based on the transport of water vapor molecules inside a hydrophobic membrane. Because of the surface tension and hydrophobic inherence of employed microporous membranes in MD technology, volatile vapor flows from the membrane to the distillate section, while the liquid isn't allowed to enter the membrane pores (Shengying et al., 2021). MD process is driven by the temperature difference formed between the feed at high temperature and the distillate. This creates a vapor pressure difference between feed and distillate solutions, which causes evaporation at the feed side of the membrane and condensation at the distillate side. This process results in a highly pure distillate solution and a concentrated feed solution where the non-volatile solutes are retained (Choi et al., 2016). Figure 14 schematically illustrates the fundamental principles of MD technology.

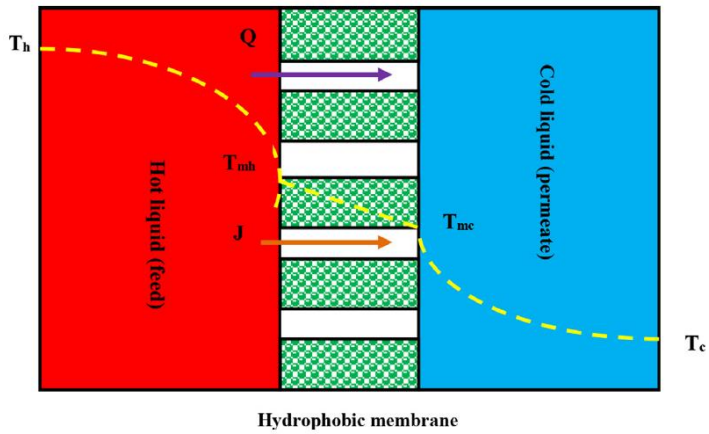

Figure 14. Fundamental principles of MD process (Shengying et al., 2021).

4.2.2 Pictures & Schematics

The MD process can be applied in four different configurations (Figure 15). These configurations differ from each other in terms of the medium in contact with the membrane at the permeate side (Alkhudhiri et al., 2012).

(i) Direct Contact MD (DCMD)

In DCMD the membrane is in direct contact with both liquid phases (feed and permeate). This is the simplest configuration and is capable of producing reasonable high flux despite its high

heat lost by conduction. It is best suited for applications such as desalination and the concentration of aqueous solutions.

(ii) Vacuum MD (VMD)

In VMD the permeate side is vapor or air under vacuum conditions. This configuration makes the heat lost conduction negligible and allows for condensation outside the membrane module. VMD is used to separate volatiles from an aqueous solution.

(iii) Air Gap MD (AGMD)

In AGMD an air gap is interposed between the membrane and the condensation surface. This configuration has the highest energy efficiency due to reduced heat lost by conduction. However, the flux obtained is generally low due to low-temperature differences across the membrane, and therefore, larger surface areas are required. The AGMD configuration can be widely employed for most MD applications, particularly where energy availability is low or in those cases where volatile compounds need to be removed from aqueous solutions.

(iv) Sweeping Gas MD (SGMD)

In SGMD a stripping inert gas is used at the permeate side to carry the vapor to condense outside the membrane module. Similarly, to AGMD, this configuration uses a gas barrier to reduce heat loss. However, in this case, the gas is not stationary, which enhances the mass transfer coefficient. In this technique, the vapor diffuses in the stripping gas as it is swept. This results in a need for a large condenser, which represents the main disadvantage of this configuration. Furthermore, an air blower or a compressor is needed to maintain the operation of this configuration, which causes an increase in both CAPEX and OPEX. SGMD configuration is suited for solutions containing volatile compounds.

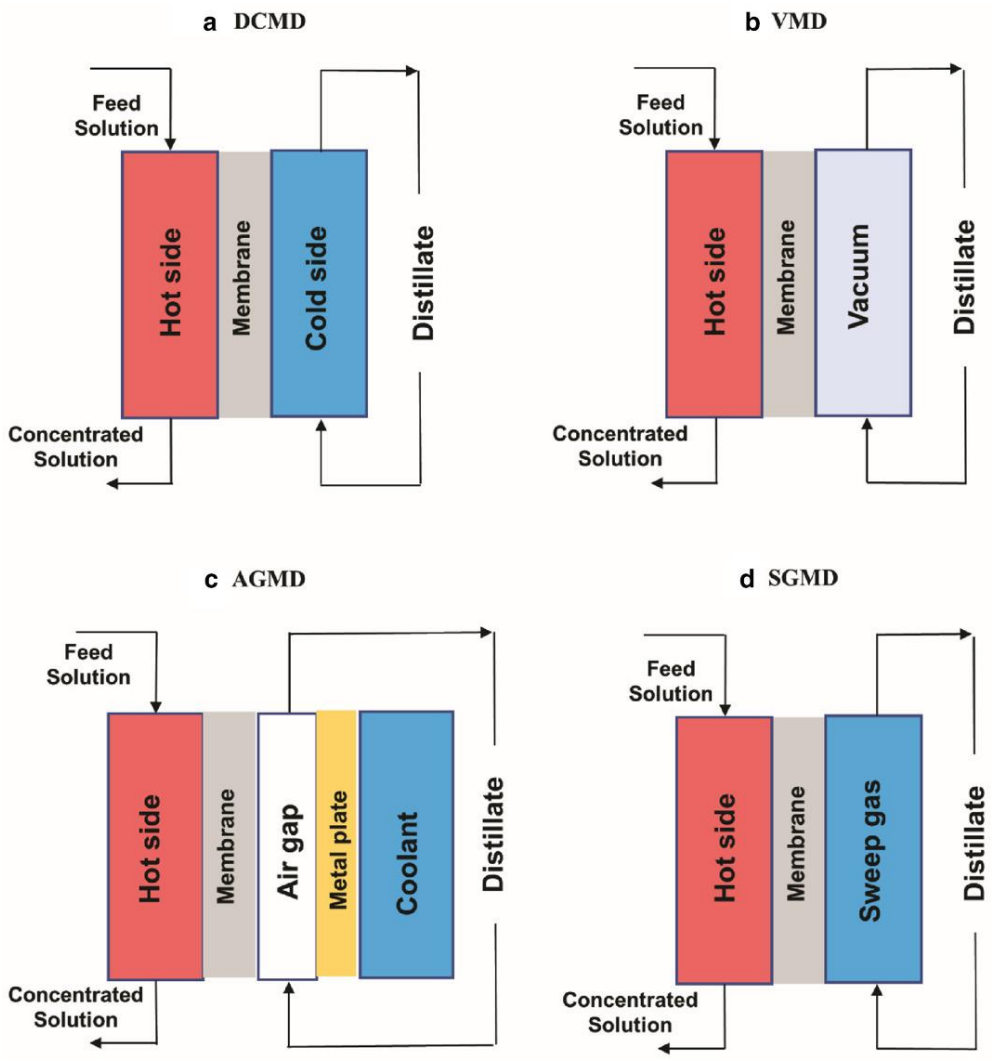

Figure 15. Schematic representation of the four major MD configurations (Pei et al., 2021)

In the framework of the WATER-MINING project, in the WP6, MD was applied to treat the brine stream from the HEXION plant, having a high temperature (85°C) at the industrial scale, to recover the organic volatile solvent Methyl isobutyl ketone (MIBK).

Solvents are an integral part of industrial processes. Almost all industrial processes rely on solvents with varying levels. The pharmaceutical industry is one of the major consumers of solvents for its active pharmaceutical ingredient (API) purification and refinement processes. Furthermore, the importance of solvents can be extended to food, cosmetics, nutraceuticals, biofuels, paints, and fine chemical industries. The continuous growth in demand for solvents has inadvertently increased waste generation. For example, approximately 25–100 kg of waste is generated per kg of a product by the pharmaceutical industry (Sheldon, 2017). The forefront of this generation issue is the inefficiencies associated with industrial processes and the poor solvent selection criteria. Undeniably, there is excessive use of solvents to achieve desired purities and quantities of products. Therefore, the increasing trends in waste solvent

generation have necessitated process intensification methods such as solvent recovery to curb the growing environmental, health, and safety concerns (Aboagye et al., 2021)

In this context, the AGMD configuration has been selected, since it shows the best performance in terms of energy efficiency and capability for latent heat recovery.

4.2.3 Description of the Experiments

4.2.3.1 Membrane distillation tests

The experimental plan was defined to evaluate the suitability of various commercial membranes for MIBK recovery out of the brine stream. The wastewater stream to treat was provided by HEXION with the characteristics enclosed in Table 14.

Table 14. Wastewater composition.

		Min	Average	Stdev	Max
Volume	kg/h		46000		
Temperature	°C	50	85	5	100
NaCl	%	7%	12%		15%
MIBK*	%		0,4%		
Epoxy Resin**	%		0,2%		
Glycerol	%		0,3%		

Before the MD tests, ultrafiltration pre-treatment was predicted to be carried out to eliminate wastewater contaminants like epoxy resin, glycerol, and polymers.

For MD experiments, a membrane distillation laboratory unit was used (Figure 16). This equipment, property of EUT, is fully automated, provides 24-hour operation, a handheld tablet for setpoints, and automatically generated .csv files for sensor values. Moreover, it also allows for building various MD configurations – DCMD, AGMD, and VMD. Other relevant characteristics are an effective membrane surface of 375 cm^2 and a condenser flow rate of 50 – 300 L/h.

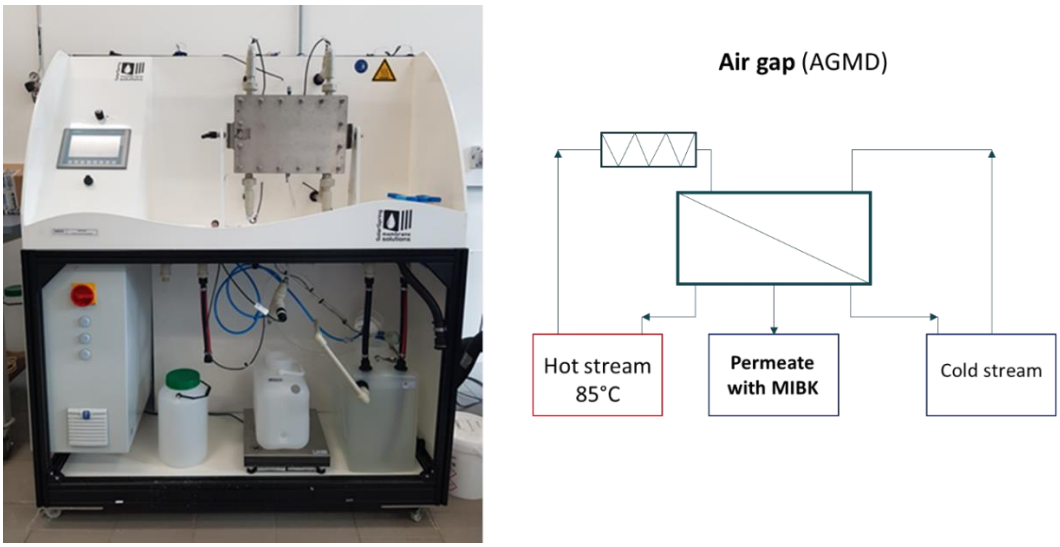

Figure 16. Membrane distillation lab equipment and schematic air gap configuration.

According to the theoretical chemical compatibility, experience, and previous results on the MD test performed by EUT for salt recovery, the hydrophobic UHMwPE (Lydall), PVDF (Sterlitech), and PTFE (SolarSpring) membranes with a pore size of 0.9, 0.1 and 0.2 µm, respectively, were selected for MD tests. To determine the temperature difference ΔT effect on the process performance, two cold stream temperatures 15°C and 25°C were selected as it corresponds to the range of the common cold water temperature. Hot stream (feed solution) temperature was determined to maintain at 85°C as it represents the real wastewater temperature at HEXION plant.

4.2.3.2 Scanning electron microscopy analysis

To evaluate real chemical and physical membrane compatibility, four small pieces (4cmx4cm) of each membrane were cut and submerged inside four small glass bottles previously filled with ultrapure water (MQ), MQ and MIBK solution (0.4%), wastewater, and MIBK solution (0.4%) and only wastewater. The twelve bottles were then placed inside a thermomixer reactor for one week at 300 rpm and 85°C (Figure 17).

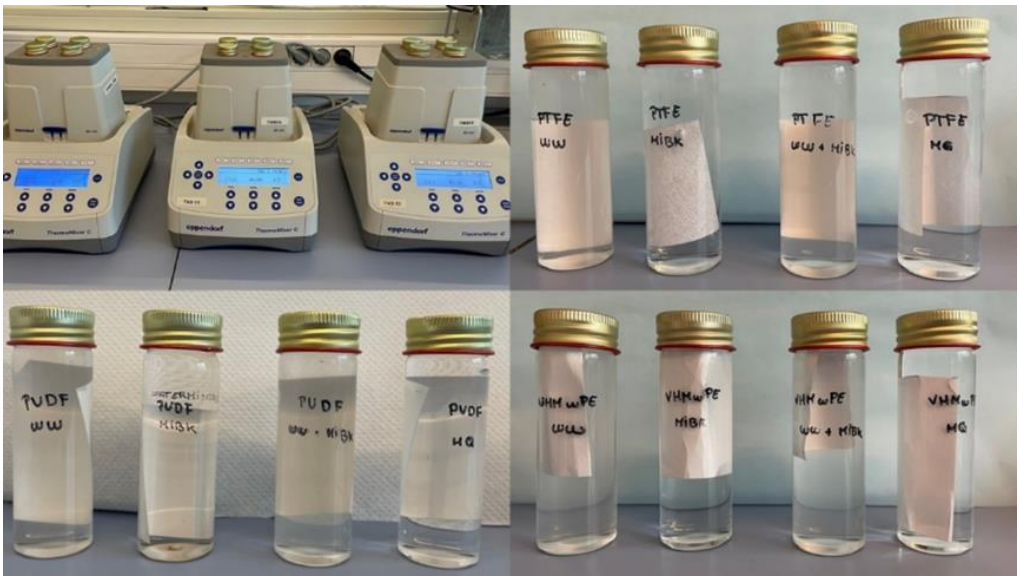

Figure 17. Thermomixer and vials with different solutions and membrane samples at the beginning of the test. After one week the membranes were withdrawn, dried and prepared for scanning electron microscope (SEM) analysis. This technique, allowing to produce high-resolution images of the membrane's surface morphology, was used to assess the effect of the wastewater and/or MIBK on the morphological properties of the membranes. Before placing membranes inside the microscope, the membrane surfaces were covered with a thin layer of gold to make membrane samples conductive. By fixing the electron beam at a single point in the membrane sample, qualitative and quantitative elemental microanalysis of the constituent elements of the specimen can be performed at that particular volume of interaction, following the method of Energy Dispersive X-Ray (EDX) spectroscopy. This SEM property allows to examine what is present on the membrane surface.

4.2.4 Results & Discussion

4.2.4.1 Membrane distillation tests

Due to challenging wastewater composition (especially glycerol and epoxy resin), a detailed literature review was performed. As a result, UF pre-treatment step before MD was rejected, because, according to the literature, the glycerol end epoxy resin elimination by UF would be insignificant or inefficient due to their molecular weight, 92.09 g/mol and 392.9 g/mol, respectively. Nevertheless, as in MD non-volatile solutions are retained, glycerol end epoxy resin with their high boiling points of 290°C and >150°C should be retained at the concentrated solution side while water and MIBK vapor should be passed the hydrophobic membrane to the permeate side as their boiling points are 100°C and 116°C, accordingly. So, MD experiments were directly performed under the conditions described above. Just after the first minutes of the experiments, unsuccessful membrane separation, provided by the MD unit conductivity sensors, were observed. The conductivity of permeate was equal to the conductivity of the feed solution 163 mS/cm meaning that dissolved salts were passing through the hydrophobic membrane. Moreover, the external appearance of the membranes after the MD test (Figure 18) also testified about the process failure.

Figure 18. ePTFE membrane´s surface after the MD test.

After these results our hypothesis was that membrane suffered pore wetting – the loss of membrane hydrophobicity due to the complex wastewater composition. When membrane wetting occurs, the electrolyte solutes dissolved in the liquid feed penetrate into membrane pores, which leads to a significant increase of permeate electrical conductivity (Warsinger et al., 2017a). Wetting phenomenon is one of the main MD drawbacks that is still challenging its industrial potential. Penetration of feed solution into the membrane pores occurs if solutions with organic or/and inorganic compounds adsorb/deposit to the membrane surface or if the transmembrane hydrostatic pressure surpasses the liquid entry pressure. Once wetting takes place, the membrane starts to lose its hydrophobicity locally, leading to continuous water bridging. Pore wetting leads to either permeate flux reduction or permeate quality deterioration depending on the type of pore wetting (Rezaei et al., 2018).

Subsequently, meetings with WP6 partners were performed, especially with HEXION team, to determine the next steps of the MD subtask. As a result, chemical and physical membrane compatibility tests were performed to point out the responsible for pore wetting during the MD experiments.

4.2.4.2 Scanning electron microscopy analysis

For easier discussion, the results of SEM analysis are presented separately for each membrane at the following sequence – PTFE, PVDF and UHMwPE. Microscope images are produced with 1X1000 zoom.

As it can be observed in Figure 19, being in contact with the PTFE membrane, MIBK solution gives an impression that did not cause severe changes in the structure of the membrane´s active surface area (Figure 19.c), appearing similar to the case of MQ water (Figure 19.a). However, after a deeper evaluation, resulted that MIBK formed like a “melted” layer on the surface of the membrane resulting in a decreased porosity. Darker and empty areas imply porosity loss, which can be distinctly observed in Figure 19.c. The solvent action with the active layer of the membrane resulted in compacting the PTFE membrane surface structure. Even being at low concentration (0.4% (w/w)), it clearly seems that MIBK solution had a modest effect to the PTFE membranes resistance. On top of that, the strongest membrane surface changes were observed when wastewater (Figure 19.b) and wastewater+MIBK solution (Figure 19.d) came into the contact with the active surface area of the PTFE membrane. These two photos markedly show potent changes in the membrane’s surface

morphology. Therefore, it is evident that wastewater composition directly impacted the MD performance, since several and diverse type of crystals formed and deposited on top of the membrane´s surface (Figure 19.b). Small “spheres” observed in Figure 19.d may be formed by the dissolved membrane material, due to the presence of MIBK and other unkonwn solvents in the wastewater matrix. This resulted in the formation of such spheric crystals and a more pronounced surface ruffness.

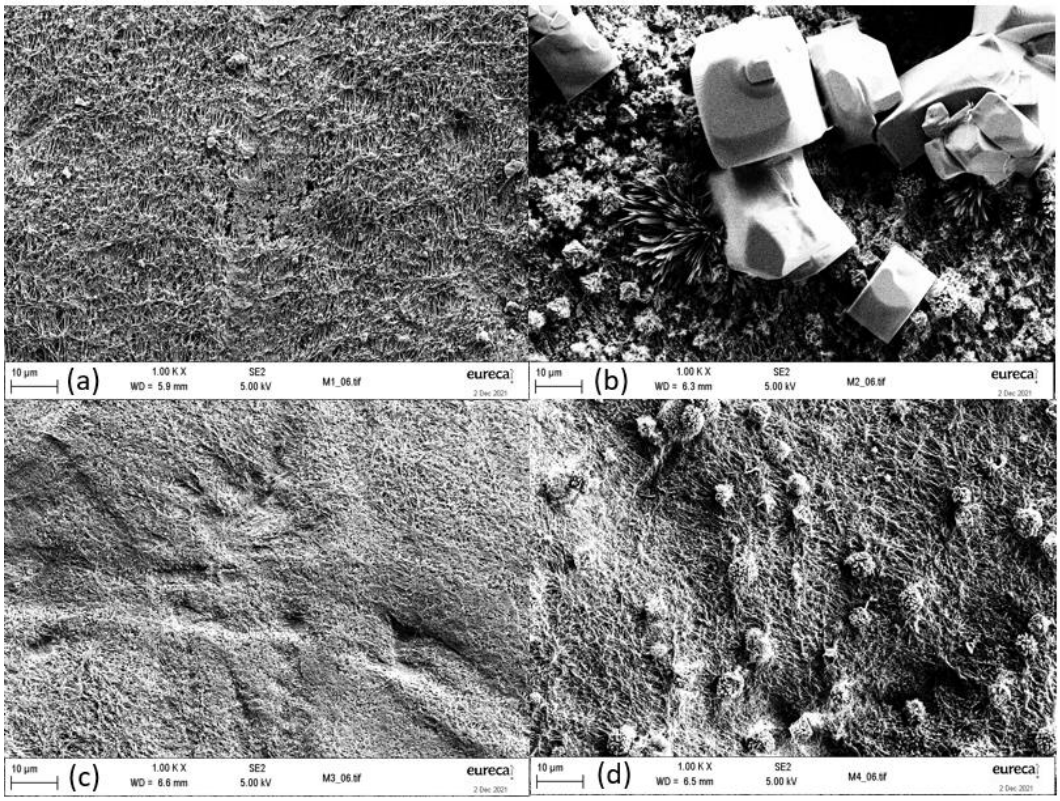

Figure 19. SEM images of PTFE membrane. (a) MQ water, (b) wastewater, (c) MQ+MIBK solution 0.4% and (d) wastewater+MIBK solution 0.4%

Through the elemental composition analysis, it was possible to estimate the main components composing those crystals (Figure 20). From the spectrum obtained by the EDX method, resulted that NaCl crystals were the dominant species, with the “almost-squared” shape clearly visible in Figure 19.b. To the same, the elemental analysis suggested that silicon dioxide was also presented on the surface of the membrane, kept in contact with the wastewater. It is interesting to highlight the shape of those dioxides since they appear like spikes able to penetrate the membrane. If this happens, then they produce a sort of bridge crossing the membrane, thus allowing the wastewater with all the other components to pass through it (Huang et al., 2017). From the evaluated spectra, the major elements that appeared on the surface of the membrane were C, O, Na, Cl, Si and Cl. The presence of fluorine can be explained by the chemical composition of the PTFE membrane which is mainly composed, among other constituents, by fluorine. Therefore F appeared in the spectrum, especially in

areas that were not entirely covered by the foulants, such as NaCl and Si-containing crystals. Spectra 10, 13, and 14 revealed the presence of silica and oxygen, forming the first layer of fouling, on top of which more foulants could be deposited and growed bigger. Moreover, the presence of Si and O suggested the presence of some siloxane (Si-O-Si), which could belonged to some polymers contained in the wastewater. According to these results, it is evident that the presence of such functional groups represented the first fouling agent, covering the surface of the membrane. To the same, the hypothesis we made was that scale deposition (inorganic fouling) was another important cause resulting in reducing the hydrophobicity of PTFE membrane.

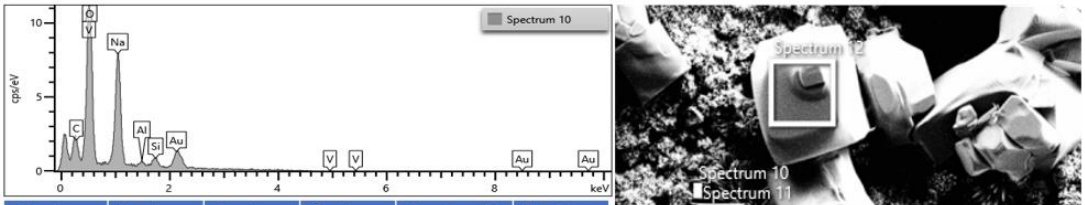

Spectrum Label	Spectrum 10	Spectrum 11	Spectrum 12	Spectrum 13	Spectrum 14
C		15.33		15.90	20.70
O	58.90	50.55	8.00	31.23	25.54
F				26.85	32.31
Na	36.95	27.91	39.63	9.62	7.19
Al					1.49
Si	4.16			16.39	12.77
Cl		6.21	52.37		
Total	100.00	100.00	100.00	100.00	100.00

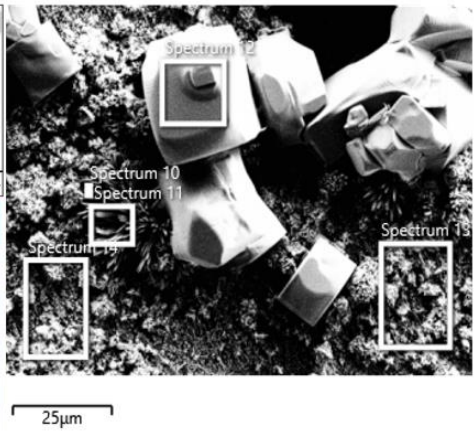

Figure 20. PTFE elemental composition analysis was carried out with EDX method.

Very similar phenomenon – severe synergistic fouling negatively affecting membranes functionality was observed for the other two membranes excluding some differences which will be highlighted as follows.

Figure 21 demonstrates the SEM images obtained for the PVDF membrane. Compared to the PTFE membrane, PVDF membrane´s active layer presented a higher solubility when only MQ+MIBK solution 0.4% was in contact with it, resulting in the appearance of some kind of "corals" on the membrane's surface (Figure 21.c). This happened due to the different nature of the PVDF polymer. To the same, according to the literature, the PVDF membrane has the lowest chemical compatibility with the MIBK in comparison to the other two membranes evaluated in this subtask.

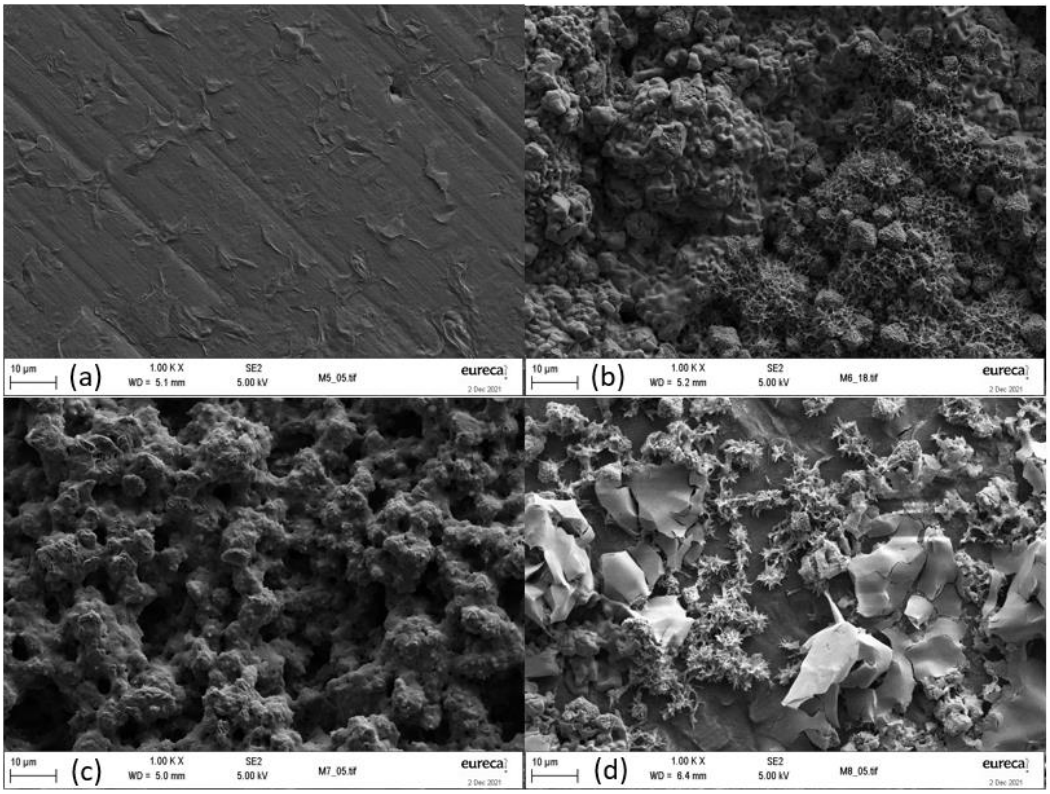

Figure 21. SEM images of PVDF membrane. (a) MQ water, (b) wastewater, (c) MQ+MIBK solution 0.4% and (d) wastewater+MIBK solution 0.4%

Further, similar to the case of PTFE, the major harm to the PVDF membrane´s active layer was caused when wastewater (Figure 21.b) and wastewater+MIBK solution 0.4% (Figure 21.d) was in contact with it. Some kind of agglomerations and crystals were observed from the SEM images, once again proving the complexity of the wastewater stream from HEXION plant. These changes in the membrane's surface morphology were again mostly caused by NaCl deposition and Si-containing polymers which led to the deterioration of the membrane´s hydrophilicity, and thus wetting (Warsinger et al., 2015). Moreover, the obvious effect of both wastewater+MIBK solution and only wastewater on PVDF membrane was visible from the visual observation of the membranes after 7 days of contact, at 85°C and 300 rpm of agitation (Figure 22).

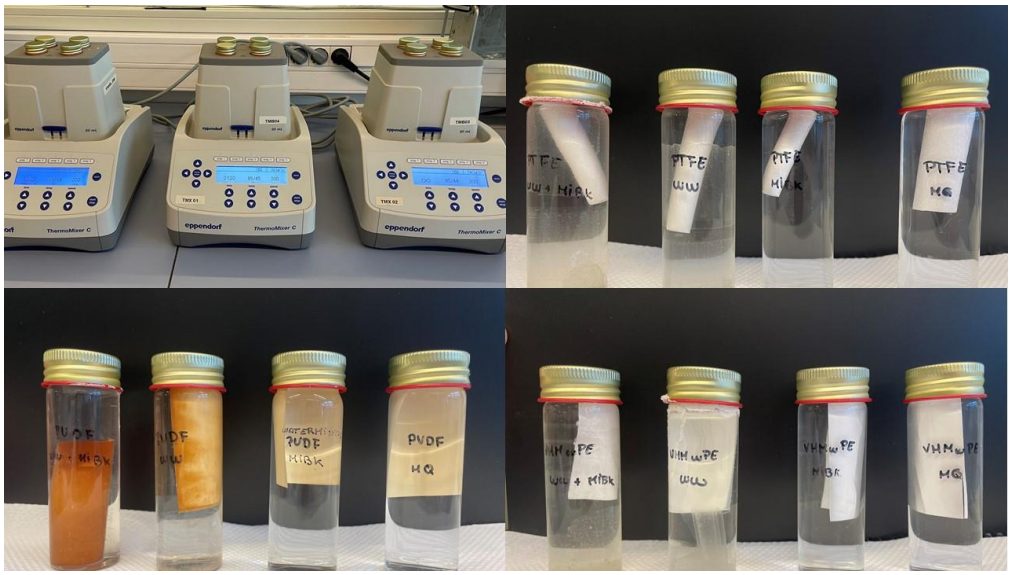

Figure 22. Thermomixer and vials with different solutions and membrane samples at the end of the test (one week later).

The polyethylene membranes, like UHMwPE, are usually used for feed solutions with the presence of solvents and polymers because they are more resistant than other membranes to such potential fouling agents. SEM images of the UHMwPE membrane (Figure 23) are in accordance to that. Slight changes were observed when the membrane was in contact with MQ+MIBK solution (Figure 23.c) whereas the membrane sample was maintained in contact with solutions containing wastewater (Figure 23.b and Figure 23.d) clearly showed formed foulants. Figure 23.b especially attracted attention due to the different structures of the foulant. On the right side of the figure, an almost uniform layer is covering the membrane surface while other parts are settled b crystals that appear as “isolated agglomerates”.

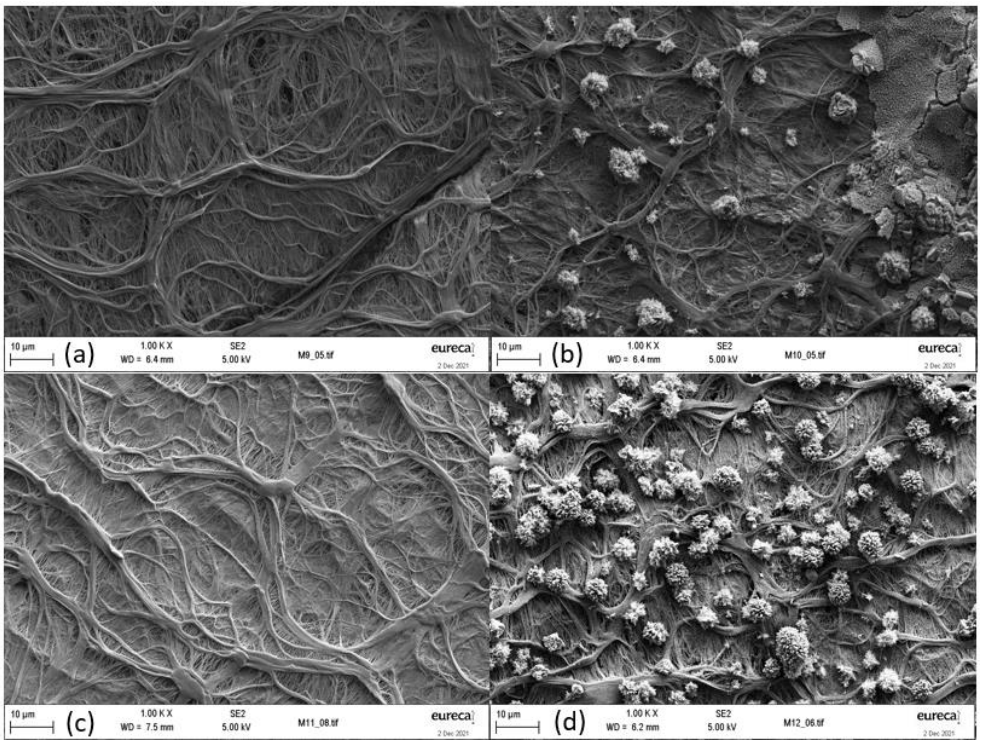

Figure 23. SEM images of UHMwPE membrane. (a) MQ water, (b) wastewater, (c) MQ+MIBK solution 0.4% and (d) wastewater+MIBK solution 0.4%

The elemental composition analysis showed that crystals deposited on the UHMwPE membrane were NaCl and Si origin as in previous cases. As explained before, these compounds are considered as fouling agents since they produce membrane wetting, thus negatively affecting the proper performance of the MD. Moreover, the elemental analysis of UHMwPE membrane suggested the presence of another chemical element that did not appear in the previous analysis for other membranes – aluminum.

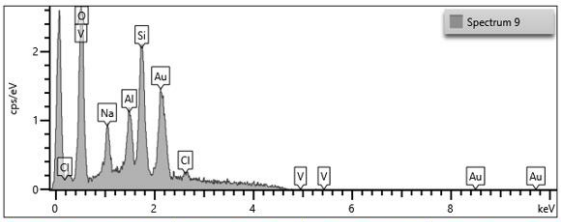

Spectrum Label	Spectrum 9	Spectrum 7	Spectrum 8
C		10.28	77.99
O	34.52	52.46	9.75
Na	10.56	4.26	2.96
Al	10.25	10.31	
Si	33.24	22.69	5.41
Cl	11.44		3.89
Sb		0.00	
Total	100.00	100.00	100.00

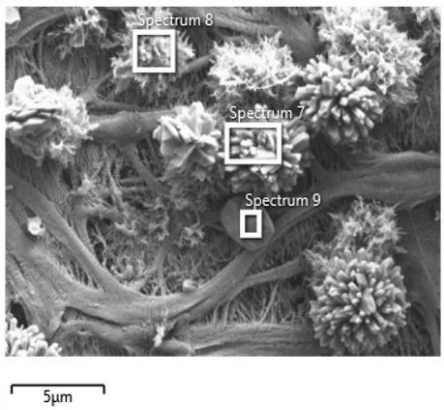

Figure 24. UHMwPE elemental composition analysis carried out with EDX method.

This inorganic component is likely one of the treated wastewater´s principles that during chemical compatibility tests resulted as inorganic colloidal foulants. The reason why these aluminum oxides did not appear in the elemental analysis of PVDF and PTFE membranes may be due to the fact that, in previous cases, there were other major fouling agents deposited on the top of the Al-containing crystals, thus blocking their appearance. According to the literature, aluminum oxide tends to result in more severe synergistic fouling compared to silicon dioxide, suggesting that the inorganic colloid material character, especially its surface charge, affects the severity of combined fouling (Schulz et al., 2016). These results definitely confirm the complexity of the wastewater stream from the HEXION plant.

4.2.5 Conclusion

In this subtask, EURECAT was intended to perform MD tests to recover MIBK solvent from the wastewater stream provided by HEXION. From the first MD trials, the separation performance resulted ineffective due to membrane pore wetting due to loss of membrane hydrophobicity, determined by an important increase in the electrical conductivity at the permeate side. Chemical and physical membrane compatibility tests were performed to point out the responsible component for pore wetting during the MD experiments. Scanning electron microscopy analysis showed significant changes in the integrity of the membrane and it was observed NaCl and Si-containing crystals as dominant fouling components for all the membranes tested. Some types of crystals, in this case Si-containing, acted like a bridge allowing the wastewater with all the other components to pass through the membrane due to their fine needle shape. Al-containing crystals were observed on the UHMwPE membrane surface demonstrating severe synergistic fouling and the complexity of the wastewater stream negatively affecting membranes functionality.

As observed within this subtask, membrane scaling and wetting, caused by complex HEXION wastewater, were two interrelated phenomena in MD. They represented significant challenges in the application of MD for MIBK separation and they were influenced by each other. The results obtained clearly demonstrated the need of strategies for wetting and fouling mitigation during wastewater treatment. To achieve it, a complete analysis and characterization has to be made for both, the wastewater produced by HEXION and the changes on the surface of the membranes by FTIR allowing to determine the source of incompatibility. In turn, evaluation of unconventional membranes is necessary for solving further chemical stability.

4.3 References

4.3.1 TU Delft: Aerobic Granular Sludge

Bassin, J. P., Pronk, M., Muyzer, G., Kleerebezem, R., Dezotti, M., & van Loosdrecht, M. C. M. (2011). Effect of elevated salt concentrations on the aerobic granular sludge process: Linking microbial activity with microbial community structure. *Applied and Environmental Microbiology*, *77*(22), 7942–7953. https://doi.org/10.1128/AEM.05016-11

Bengtsson, S., de Blois, M., Wilén, B. M., & Gustavsson, D. (2018). Treatment of municipal wastewater with aerobic granular sludge. *Critical Reviews in Environmental Science and Technology*, *48*(2), 119–166. https://doi.org/10.1080/10643389.2018.1439653

Coats, E. R., Dobroth, Z. T., & Brinkman, C. K. (2015). EBPR Using Crude Glycerol: Assessing Process Resiliency and Exploring Metabolic Anomalies. *Water Environment Research*, *87*(1), 68–79. https://doi.org/10.2175/106143014x14062131179113

Corsino, S. F., Campo, R., Di Bella, G., Torregrossa, M., & Viviani, G. (2015). Cultivation of granular sludge with hypersaline oily wastewater. *International Biodeterioration and Biodegradation*, *105*, 192–202. https://doi.org/10.1016/j.ibiod.2015.09.009

de Graaff, D. R., van Loosdrecht, M. C. M., & Pronk, M. (2020). Biological phosphorus removal in seawater-adapted aerobic granular sludge. *Water Research*, *172*, 115531. https://doi.org/10.1016/j.watres.2020.115531

de Kreuk, M. K., Pronk, M., & van Loosdrecht, M. C. . (2005). *Formation of aerobic granules and conversion processes in an aerobic granular sludge reactor at moderate and low temperatures*. Water Research. https://reader.elsevier.com/reader/sd/pii/S0043135405005063?token=9032909210B6C90B9950D06D3177DEE4ECCA1E459F4772B4FFC4EA37375730B3A4E0630464FE3F645FB1479C37D6CE08&originRegion=eu-west-1&originCreation=20210816085711

de Kreuk, M. K., & van Loosdrecht, M. C. M. (2004). Selection of slow growing organisms as a means for improving aerobic granular sludge stability. *Water Science and Technology*, *49*(11–12), 9–17. https://doi.org/10.2166/wst.2004.0792

Felz, S., Al-Zuhairy, S., Aarstad, O. A., van Loosdrecht, M. C. M., & Lin, Y. M. (2016). Extraction of structural extracellular polymeric substances from aerobic granular sludge. *Journal of Visualized Experiments*, *2016*(115), 1–8. https://doi.org/10.3791/54534

Guerrero, J., Guisasola, A., & Baeza, J. A. (2015). *Controlled crude glycerol dosage to prevent EBPR failures in C/N/P removal WWTPs*. https://doi.org/10.1016/j.cej.2015.02.062

Guerrero, J., Tayà, C., Guisasola, A., & Baeza, J. A. (2012). Glycerol as a sole carbon source for enhanced biological phosphorus removal. *Water Research*, *46*(9), 2983–2991. https://doi.org/10.1016/j.watres.2012.02.043

Haaksman, V. A., Mirghorayshi, M., van Loosdrecht, M. C. M., & Pronk, M. (2020). Impact of aerobic availability of readily biodegradable COD on morphological stability of aerobic granular sludge. *Water Research*, *187*(September), 116402. https://doi.org/10.1016/j.watres.2020.116402

Ibrahim, A., Hiripitiyage, Y., Peltier, E., & Sturm, B. S. M. (2020). Use of Halophilic Bacteria to Improve Aerobic Granular Sludge Integrity in Hypersaline Wastewaters. *Environmental Engineering Science*, *37*(5), 306–315. https://doi.org/10.1089/ees.2019.0349

Mery-Araya, C., Lear, G., Perez-Garcia, O., Astudillo-Garcia, C., & Singhal, N. (2019). Using carbon substrate as a selection pressure to enhance the potential of aerobic granular sludge microbial communities for removing contaminants of emerging concern. *Bioresource Technology*, *290*(June), 121705. https://doi.org/10.1016/j.biortech.2019.121705

Oehmen, A., Lemos, P. C., Carvalho, G., Yuan, Z., Blackall, L. L., & Reis, M. A. M. (2007). *Advances in enhanced biological phosphorus removal : From micro to macro scale*. *41*, 2271–2300. https://doi.org/10.1016/j.watres.2007.02.030

Oehmen, A., Yuan, Z., Blackall, L. L., & Keller, J. (2005). Comparison of acetate and propionate uptake by polyphosphate accumulating organisms and glycogen accumulating organisms. *Biotechnology and Bioengineering*, *91*(2), 162–168. https://doi.org/10.1002/bit.20500

Pinto, B. P., & De Araujo Mota, C. J. (2014). Developments in glycerol byproduct-based biorefineries. *Advances in Biorefineries: Biomass and Waste Supply Chain Exploitation*, 364–385. https://doi.org/10.1533/9780857097385.1.364

Plácido, J., & Capareda, S. (2016). Conversion of residues and by-products from the biodiesel industry into value-added products. *Bioresources and Bioprocessing 2016 3:1*, *3*(1), 1–12. https://doi.org/10.1186/S40643-016-0100-1

Pronk, M., Abbas, B., Al-zuhairy, S. H. K., Kraan, R., Kleerebezem, R., & van Loosdrecht, M. C. M. (2015). Effect and behaviour of different substrates in relation to the formation of aerobic granular sludge. *Applied Microbiology and Biotechnology*, *99*(12), 5257–5268. https://doi.org/10.1007/s00253-014-6358-3

Sarvajith, M., & Nancharaiah, Y. V. (2020). *Biological nutrient removal by halophilic AGS under hypersaline seawater conditions.pdf*.

Smyk, J., & Ignatowicz, K. (2017). The influence of glycerin on nitrogen removal in wastewater treatment with activated sludge. *E3S Web of Conferences*, *22*. https://doi.org/10.1051/E3SCONF/20172200161

Winkler, M. K. H., Kleerebezem, R., De Bruin, L. M. M., Verheijen, P. J. T., Abbas, B., Habermacher, J., Van Loosdrecht, M. C. M., MKH, W., R, K., LMM, de B., PJT, V., B, A., J, H., & MCM, van L. (2013). Microbial diversity differences within aerobic granular sludge

and activated sludge flocs. *Applied Microbiology and Biotechnology*, *97*(16), 7447–7458. https://doi.org/10.1007/s00253-012-4472-7

Yang, G., Wang, D., Yang, Q., Zhao, J., Liu, Y., Wang, Q., Zeng, G., Li, X., & Li, H. (2018). Effect of acetate to glycerol ratio on enhanced biological phosphorus removal. *Chemosphere*, *196*, 78–86. https://doi.org/10.1016/j.chemosphere.2017.12.167

Zeng, J., Gao, J. M., Chen, Y. P., Yan, P., Dong, Y., Shen, Y., Guo, J. S., Zeng, N., & Zhang, P. (2016). Composition and aggregation of extracellular polymeric substances (EPS) in

4.3.2 Eurecat: Membrane Distillation

Aboagye, E.A., Chea, J.D., Yenkie, K.M. (2021). Systems level roadmap for solvent recovery and reuse in industries. Review. iScience 24, 103–114.

Alkhudhiri, A., Darwish, N., & Hilal, N. (2012). Membrane distillation: A comprehensive review. Desalination, 287, 2–18.

Huang, Y. X., Wang, Z., Jin, J., & Lin, S. (2017). Novel Janus Membrane for Membrane Distillation with Simultaneous Fouling and Wetting Resistance. Environmental Science and Technology, 51(22), 13304–13310.

Pei, J., Gao, S., Sarp, S., Wang, H., Chen, X., Yu, J., … Li, Z. (2021). Emerging forward osmosis and membrane distillation for liquid food concentration: A review. Comprehensive Reviews in Food Science and Food Safety, 20(2), 1910–1936.

Rezaei, M., Warsinger, D. M., Lienhard V, J. H., Duke, M. C., Matsuura, T., & Samhaber, W. M. (2018). Wetting phenomena in membrane distillation: Mechanisms, reversal, and prevention. Water Research, 139, 329–352.

Schulz, M., Soltani, A., Zheng, X., Ernst, M. (2016). Effect of inorganic colloidal water constituents on combined low-pressure membrane fouling with natural organic matter (NOM). Journal of Membrane Science 507.

Sheldon, R.A. (2017). The E factor 25 years on: the rise of green chemistry and sustainability. Green. Chem. 19, 18–43.

Shengying, Y., Saade Abdalkareem, J., Bokov, D., Chupradit, S., Taghvaie Nakhjiri, A., El-Shafay, A.S. (2021). Membrane distillation technology for molecular separation: A review on the fouling, wetting and transport phenomena. Journal of Molecular Liquids, 118–115.

Warsinger, D. M., Swaminathan, J., Guillen-Burrieza, E., Arafat, H. A., & Lienhard V, J. H. (2015). Scaling and fouling in membrane distillation for desalination applications: A review. In Desalination 356, pp. 294–313.

Warsinger, D.M., Servi, A., Connors, G.B., Mavukkandy, M.O., Arafat, H.A., Gleason, K.K., Lienhard, J.H. (2017a). Reversing membrane wetting in membrane distillation: comparing dryout to backwashing with pressurized air. Environ. Sci. Water Res. Technol. 3, 930–939.